Multiphonon resonant Raman scattering in the semimagnetic semiconductor $Cd_{1-x}Mn_xTe$: Fröhlich and deformation potential exciton–phonon interaction

2003 J. Phys.: Condens. Matter 15 3225

(http://iopscience.iop.org/0953-8984/15/19/323)

INSTITUTE OF PHYSICS PUBLISHING JOURNAL OF PHYSICS: CONDENSED MATTER

J. Phys.: Condens. Matter **15** (2003) 3225–3248 PII: S0953-8984(03)53278-7

Multiphonon resonant Raman scattering in the semimagnetic semiconductor $Cd_{1-x}Mn_xTe$: Fröhlich and deformation potential exciton–phonon interaction

R Riera[1], R Rosas[1], J L Marín[2], J M Bergues[2,3] and G Campoy[2]

[1] Departamento de Física, Universidad de Sonora, Apartado Postal 1626, 83000 Hermosillo, Sonora, Mexico
[2] Centro de Investigación en Física, Universidad de Sonora, Apartado Postal 5-088, 83190 Hermosillo, Sonora, Mexico

Received 11 September 2002, in final form 24 February 2003
Published 6 May 2003
Online at stacks.iop.org/JPhysCM/15/3225

Abstract

A theory describing multiphonon resonant Raman scattering (MPRRS) processes in wide-gap diluted magnetic semiconductors is presented, with $Cd_{1-x}Mn_xTe$ as an example. The incident radiation frequency ω_l is taken above the fundamental absorption region. The photoexcited electron and hole make real transitions through the LO phonon, when one considers Fröhlich (F) and deformation potential (DP) interactions. The strong exchange interaction, typical of these materials, leads to a large spin splitting of the exciton states in the magnetic field. Neglecting Landau quantization, this Zeeman splitting gives rise to the formation of eight bands (two conduction and six valence ones) and ten different exciton states according to the polarization of the incident light. Explicit expressions for the MPRRS intensity of second and third order, the indirect creation and annihilation probabilities, the exciton lifetime, and the probabilities of transition between different exciton states and different types of exciton as a function of ω_l and the external magnetic field are presented. The selection rules for all hot exciton transitions via exciton–photon interaction and F and DP exciton–phonon interactions are investigated. The exciton energies, as a function of B, the Mn concentration x, and the temperature T, are compared to a theoretical expression. Graphics for creation and annihilation probabilities, lifetime, and Raman intensity of second and third order are discussed.

1. Introduction

The multiphonon Raman scattering technique has become suitable for the investigation of both electronic states and their interaction with the longitudinal oscillations of the lattice in

[3] On leave from: Department of Physics, Oriente University, Santiago de Cuba, Cuba.

0953-8984/03/193225+24$30.00

semiconductors, allowing us to obtain the dispersion law for the phonons over a great range inside the Brillouin zone. Through measuring the relation of the intensities I_{n+1}/I_n of two successive lines in the spectrum, one can evaluate the exciton–phonon coupling constant.

In the last few years, a great number of publications have been devoted to studying the physics of ternary II–VI and III–V semiconductor alloys; this is because of the multiple applications of these materials in new electronic and optoelectronic devices. In diluted magnetic or semimagnetic semiconductors, such as the ternary alloy $Cd_{1-x}Mn_xTe$, some of the cations are randomly replaced by transition-metal ions with permanent magnetic moments [1, 2]. Local magnetic spin moments of Mn^{+2} ions arise from the $3d^5$ electrons and strongly interact with the electrons or holes in the conduction and valence bands, producing a variety of significant phenomena in optical processes. The presence of an external magnetic field leads to extremely large magneto-optical effects such as giant Zeeman splitting of the excitonic band, large Faraday rotation, giant Stokes shift in spin-flip Raman scattering [1], and the formation of so-called exciton magnetic polarons [3–5].

In view of the growing interest in diluted magnetic semiconductors (DMS), such as $Cd_{1-x}Mn_xTe$, and their interesting physical properties, it has become important to investigate them by different techniques, such as by studying the high-order Raman scattering. Therefore, it is important to construct a theoretical model for this phenomenon in order to obtain information, by comparing with the experimental results, about properties such as the exciton lifetime, the Landé g-factor, and the exchange integral for these interesting semiconductors.

When light with energy in the region of the fundamental absorption interacts with a polar semiconductor (especially one of the type II–VI), the scattered light contains a set of lines differing in energy from that of the incident light, $\hbar\omega_l$, by an integer number $N \geqslant 2$ times the energy of an LO phonon. That is, $\hbar\omega_s = \hbar\omega_l - N\hbar\omega_{LO}$, where $\hbar\omega_s$ is the energy of the scattered photon and $\hbar\omega_{LO}$ is that of a LO (longitudinal optical) phonon. These results have been interpreted as multiphonon Raman resonant scattering [6–9]. Recently, MPRRS in III–VII semiconductors, such as InBr and InI, has been studied. In these materials, electron and hole effective masses are supposed to have nearly the same value. In this case, a great number of MPRRS lines with alternating intensity (N-even lines brighter than N-odd ones) were observed [10–13]. The MPRRS processes involving free electron–hole pairs (without Coulomb interaction) have also been investigated, in the presence of an external strong magnetic field with direct creation and indirect annihilation of electron–hole pairs when $m_e \neq m_h$, and with direct creation and direct annihilation of electron–hole pairs with $m_e \neq m_h$. Additionally, the second-order Raman scattering for the $m_e = m_h$ case when direct creation and direct annihilation are allowed has also been investigated [14].

A theory for one-phonon resonant Raman scattering in wide-gap DMS is developed in [15], where the efficiency of resonant Raman scattering by LO phonons via deformation potential (DP) and Fröhlich (F) exciton–phonon interaction near the E_0-gap in external magnetic fields in $Cd_{1-x}Mn_xTe$ is calculated. At the present time, we do not know of any theoretical or experimental studies carried out on MPRRS processes in the DMS. The aim of this work is to investigate MPRRS processes in DMS in the presence of an external magnetic field, with $Cd_{1-x}Mn_xTe$ as an example. The presence of an external magnetic field generates two conduction bands and six valence bands with ten different types of exciton. The Zeeman splitting and exciton states are considered in the envelope function approximation using a parabolic and isotropic model near $k = 0$ for the conduction and valence bands. Theoretical expressions for the MPRRS cross-section will be obtained, and selection rules will be discussed for all exciton transitions by LO phonons via F and DP exciton–phonon interaction. As a starting point we use the results of the following two references:

(a) Reference [15], where the absolute Raman scattering efficiency for one-phonon resonant scattering processes via DP and F exciton–phonon interaction in DMS, with $Cd_{1-x}Mn_xTe$ as an example, has been calculated for photon energies below and above the band gaps E_0 and $E_0 + \Delta_0$. In this reference the fundamental properties related to the structure of bands and transitions allowed for polarization vectors of the incident radiation field in the DMS are given.
(b) Reference [16], where a theory is developed which describes MPRRS processes in polar semiconductor with two exciton bands when the incident radiation frequency is above the fundamental absorption region.

In this work the MPRRS for hot excitons will be generalized in order to allow application to the DMS; furthermore, the presence of a moderate magnetic field will be considered. A theoretical model which describes, qualitatively at least, the high-order light scattering processes in these semiconductors will be constructed. Additionally, we will present the different probabilities and the lifetimes of hot excitons involved in the process. To do this, we will take it into account that the intermediate states are real hot excitons coupled with phonons via the F and the DP interactions.

2. The model for exciton bands in diluted magnetic semiconductors

The main property of the DMS is that the Landau quantization [19] is not observed for magnetic field $B < 10$ T. Therefore, it is not necessary to include the magnetic field in the initial Hamiltonian describing the hot exciton states; that is, it will be enough to consider that the magnetic field affects the excitonic states through the energy gap.

In this section, we will consider the band model presented in [15], where, considering only the Zeeman effect (Landau quantization is neglected), the Γ_6^c conduction band is split into two bands with spin up, $|1/2, 1/2\rangle$, and down, $|1/2, -1/2\rangle$. The Γ_8^v valence bands are split into four bands, $|3/2, \pm 3/2\rangle$ and $|3/2, \pm 1/2\rangle$. The Γ_7^s band is split into two bands, $|1/2, \pm 1/2\rangle$. In the above notation the first number corresponds to the total angular momentum J_α (where α is e or h) and the second one to the z-component.

The energies of these states, in the mean-field approximation, can be written as follows [17] ($\kappa = 0$):

$$\begin{aligned} E_c[J_e = \tfrac{1}{2}, J_{ze} = \pm\tfrac{1}{2}] &= E_0 \pm 3A_e, \\ E_v[J_h = \tfrac{3}{2}, J_{zh} = \pm\tfrac{3}{2}] &= \pm 3A_h, \\ E_v[J_h = \tfrac{3}{2}, J_{zh} = \pm\tfrac{1}{2}] &= \pm A_h, \\ E_v[J_h = \tfrac{1}{2}, J_{zh} = \pm\tfrac{1}{2}] &= \mp A_h - \Delta_0, \end{aligned} \tag{1}$$

with A_e and A_h given by

$$A_e = \tfrac{1}{6}N_0 x\alpha\langle S_z\rangle_{B,T}, \qquad A_h = \tfrac{1}{6}N_0 x\beta\langle S_z\rangle_{B,T}, \tag{2}$$

where N_0 is the number of primitive cells per unit volume, x is the Mn mole fraction and $\alpha > 0$ and $\beta < 0$ are the exchange integrals for the conduction and valence band, respectively. $\langle S_z\rangle_{B,T}$ is the average spin polarization of Mn^{2+} ions in the direction of the applied magnetic field; it has been found [18] that for $B < 10$ T, for $Cd_{1-x}Mn_xTe$, this magnitude can be described by the modified Brillouin function $B_s(t)$ with $S = 5/2$ (the total spin of $3d^5$ electrons) as follows:

$$\begin{aligned} \langle S_z\rangle_{B,T} &= S_0 B_s\left(\frac{S\mu_\beta g B}{k_B(T + T_0)}\right), \\ B_s(r) &= \frac{2S+1}{2S}\coth\left(\frac{(2S+1)}{2S}r\right) - \frac{1}{2S}\coth\left(\frac{r}{2S}\right), \end{aligned} \tag{3}$$

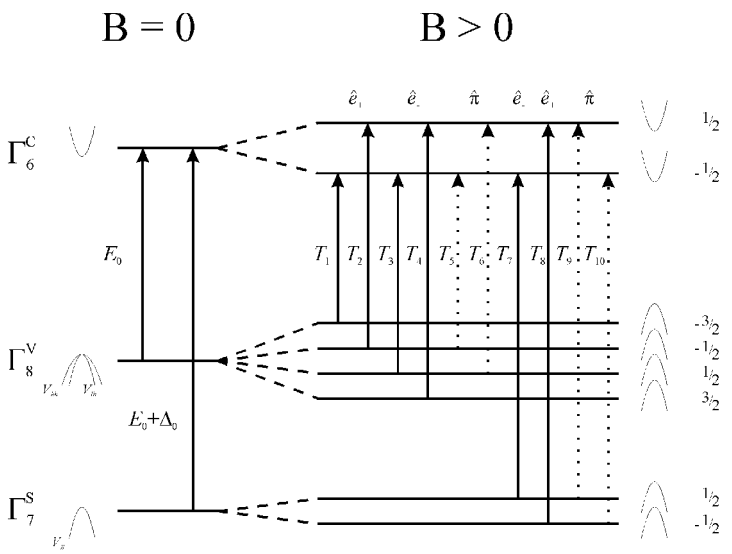

Figure 1. A schematic representation of the band structure without the presence of a magnetic field. Zeeman-like splitting of the Γ_6^c conduction and Γ_7^s, Γ_8^v valence band states, at $\boldsymbol{k} = 0$, for a zinc-blende-type DMS in external magnetic fields are also shown. Transitions allowed for polarization vectors $\hat{e}_+$ (T_1, T_2, T_8) and $\hat{e}_-$ (T_3, T_4, T_7) are indicated by solid arrows, while those allowed for the polarization vector $\hat{\pi}$ (T_5, T_6, T_9, T_{10}) are shown by dashed arrows.

where S_0 and T_0 are empirical parameters, μ_B is the Bohr magneton, and g is the Landé factor for Mn^{2+} ions. The variations of T and B allow us to adjust the exciton bands for a given concentration x of the Mn^{2+} ions.

In figure 1 we show the Zeeman-like splitting of the Γ_6^c conduction and Γ_7^s and Γ_8^v valence band states at $\kappa = 0$ for zinc-blende-type DMS, with and without external magnetic fields. The allowed transitions for the polarization vector $\hat{e}_+$ (T_1, T_2, T_8) and $\hat{e}_-$ (T_3, T_4, T_7) are indicated by solid arrows, and those allowed for the polarization vector $\hat{\pi}$ (T_5, T_6, T_9, T_{10}) are shown by dashed arrows; the polarization vectors are given by

$$\hat{e}_+ = \frac{1}{\sqrt{2}}(1, \mathrm{i}, 0), \qquad \hat{e}_- = \frac{1}{\sqrt{2}}(1, -\mathrm{i}, 0). \tag{4}$$

In zinc-blende-type DMS the exchange interaction is diagonal in the basis of the total angular momentum wavefunctions $|J, J_z\rangle$ and does not mix the states with different J_z [15, 19]. The coulombic interaction between electrons and holes leads to the formation of exciton states downshifted with respect to the threshold interband transitions by the binding energy E_R. For $Cd_{1-x}Mn_xTe$ the difference in binding energy is very small for different exciton states and, neglecting effects of electron–hole exchange, the exciton spin splitting can be written as algebraic sums of valence and conduction band splittings. Only six exciton transitions (T_1, T_2, T_3, T_4, T_7, T_8) are allowed in the Faraday configuration [15, 19]. The energies of these states in the centre of the Brillouin zone and in the internal ground state are

$$\begin{aligned}
T_1 &= E_0 - \Delta E + 3A_h - 3A_e,\\
T_2 &= E_0 - \Delta E + A_h + 3A_e,\\
T_8 &= E_0 + \Delta_0 - \Delta E - A_h + 3A_e,\\
T_3 &= E_0 - \Delta E - A_h - 3A_e,\\
T_4 &= E_0 - \Delta E - 3A_h + 3A_e,\\
T_7 &= E_0 + \Delta_0 - \Delta E + A_h - 3A_e,
\end{aligned} \tag{5}$$

where $\Delta E = R_p/n^2$ is the binding energy of the p-exciton for the discrete spectrum; we have considered the ground state ($n = 1$).

The first three transitions are allowed in the $\hat{e}_+$-polarization and the last three in the $\hat{e}_-$-polarization.

In general, the different excitonic transitions via F exciton–phonon interaction are intraband transitions for q-excitons in the MPRRS processes. Therefore, the transitions mediated by F interaction are possible with $Z(\hat{e}_\pm, \hat{e}_\pm)\bar{Z}$ scattering configurations. Both configurations will be taken into account in the calculation of the MPRRS cross-section in DMS.

3. Exciton–phonon interaction

In DMS there are two types of interaction contributing to the emission of a LO phonon by an exciton; these are the DP interaction [30] and the F [31] interaction. Both interactions can produce interband and intraband transitions if the phonon momentum is $Q \neq 0$. The Hamiltonian for the exciton–phonon interaction for Stokes processes is given by

$$\hat{H}_{eph} = \sum_{\substack{p,\nu,\boldsymbol{K},\boldsymbol{Q},\lambda \\ q,\nu',\boldsymbol{K}'}} G^{\boldsymbol{K}\boldsymbol{K}'}_{p\nu,q\nu'}(\boldsymbol{Q})\hat{D}^+_{q,\nu',\boldsymbol{K}'}\hat{D}_{p,\nu,\boldsymbol{K}}\hat{b}^+_{\boldsymbol{Q},\lambda}, \tag{6}$$

where $\boldsymbol{Q}$ is the wavevector of a phonon, λ is the phonon branch, $\hat{D}^+_{q,\nu',\boldsymbol{K}'}$ ($\hat{D}_{p,\nu,\boldsymbol{K}}$), is the creation (annihilation) operator for an exciton q (p) with quantum number ν' (ν), centre-of-mass momentum $\boldsymbol{K}'$ ($\boldsymbol{K}$) and energy $E_{q,\nu'}(\boldsymbol{K}')$ ($E_{q,\nu}(\boldsymbol{K})$), and $\hat{b}^+_{\boldsymbol{Q},\lambda}$ is the creation operator for phonons.

Hereafter we only will take into account the most strongly contributing optical longitudinal oscillations, considering the resonance condition; that is, the different intermediate states are resonant. The necessary condition for intermediate excitonic states to be resonant is given by equation (33).

The exciton-coupling constant of the exciton–phonon interaction can be expressed as [15]

$$\begin{aligned} G^{\boldsymbol{K}\boldsymbol{K}'}_{p\nu,q\nu'}(\boldsymbol{Q}) = \{&\langle c_q|\delta\phi^{(\lambda)}|c_p\rangle\delta_{v_q,v_p}I_{p\nu,q\nu'}(-\boldsymbol{Q}_{h,p}) \\ &- \langle v_p|\delta\phi^{(\lambda)}|v_q\rangle\delta_{c_q,c_p}I_{p\nu,q\nu'}[\tfrac{1}{2}(\boldsymbol{Q}_{e,p} + \boldsymbol{Q}_{e,q})]\}\delta_{\boldsymbol{K},\boldsymbol{K}'+\boldsymbol{Q}} \end{aligned} \tag{7}$$

where

$$\boldsymbol{Q}_{e,p} = \frac{m_e}{m_e + m_{h,p}}\boldsymbol{Q}a_p, \qquad \boldsymbol{Q}_{h,p} = \frac{m_{h,p}}{m_e + m_{h,p}}\boldsymbol{Q}a_p; \tag{8}$$

where a_p is the p-exciton Bohr radius, $I_{p\nu,q\nu'}(\boldsymbol{Q})$ is equal to

$$I_{p\nu,q\nu'}(\boldsymbol{Q}) = \int \mathrm{d}^3r\, \Psi^*_{q,\nu'}(\boldsymbol{r})\mathrm{e}^{\mathrm{i}\boldsymbol{Q}\cdot\boldsymbol{r}}\Psi_{p,\nu}(\boldsymbol{r}) \tag{9}$$

and

$$\delta\phi^{(\lambda)} = \delta\phi^{(\lambda)}_{DP} + \delta\phi^{(\lambda)}_{F}\delta_{\lambda,LO} \tag{10}$$

with subscript λ standing for subscripts LO, TO.

In the case of scattering of LO phonons via DP interaction,

$$\delta^{(LO)}_{DP} = \hat{\boldsymbol{e}}_{LO}\cdot\boldsymbol{u}_0\frac{\partial V_{eff}}{\partial u_{rel}}, \tag{11}$$

where $\hat{e}_{LO}$ is the polarization vector of the LO phonon, $\partial V_{eff}/\partial u_{rel}$ is the derivative of the effective electronic potential V_{eff} with respect to a relative sublattice displacement u_{rel}. The zero-point relative displacement amplitude u_0 is

$$u_0 = \left(\frac{\hbar V_c}{2VM^*\omega_0}\right), \tag{12}$$

where V_c is the volume of the primitive cell, M^* is the reduced mass of the atoms contributing to the optical mode, ω_0 is the phonon frequency, and V is the volume of the crystal.

For the F exciton–phonon interaction we obtain

$$\delta_F^{(LO)} = \frac{1}{\sqrt{V}} \frac{C_F}{Q} \hat{e}_{LO} \cdot \boldsymbol{Q}; \tag{13}$$

where C_F is the F constant, given by

$$C_F = -\mathrm{i}\sqrt{2\pi\hbar\omega_0 e^2(\varepsilon_\infty^{-1} - \varepsilon_0^{-1})}; \tag{14}$$

e is the free electron charge and ε_∞ and ε_0 are the high-frequency and the static dielectric constants, respectively.

In order to evaluate the integral $I_{p\nu,q\nu'}(\boldsymbol{Q})$ for discrete–discrete transitions we use the wavefunctions with angular momentum $l = 0$ for two different excitons, given by [29]

$$\Psi_{p,\nu}(\boldsymbol{r}) = \frac{1}{(\pi\nu^3 a_p^3)^{1/2}} \exp\left(-\frac{\boldsymbol{r}}{\nu a_p}\right) F\left(1-\nu, 2, \frac{2r}{\nu a_p}\right) \tag{15}$$

and

$$\Psi_{q,\nu'}(\boldsymbol{r}) = \frac{1}{(\pi\nu'^3 a_q^3)^{1/2}} \exp\left(-\frac{\boldsymbol{r}}{\nu' a_q}\right) F\left(1-\nu', 2, \frac{2r}{\nu' a_q}\right), \tag{16}$$

where F is the confluent hypergeometric function.

After very cumbersome calculations we obtain

$$\begin{aligned} I_{p\nu,q\nu'}(\boldsymbol{Q}) = {} & \frac{4(-1)^{\nu'-1}(\nu'\nu f_{qp})^{3/2} F(1-\nu', 1-\nu, 2, \frac{-4\nu'\nu f_{qp}}{(\nu-\nu' f_{qp})^2+Q'^2})}{Q'[(\nu-\nu' f_{qp})^2+Q'^2][(\nu+\nu' f_{qp})^2+Q'^2]^{\nu'+\nu}} \operatorname{Im}\{[\nu^2-(\nu' f_{qp})^2 \\ & - Q'(Q'-2\mathrm{i}\nu)]^{\nu'}[\nu^2-(\nu' f_{qp})^2+Q'(Q'-2\mathrm{i}\nu')]^{\nu}\} \end{aligned} \tag{17}$$

where $f_{qp} = a_q/a_p$ and $Q' = \nu\nu' a_q \mu_{q\alpha} Q$, where $\mu_{q\alpha}$ is the reduced mass of exciton q.

Expanding the imaginary term and keeping only the lower powers of Q' in this expansion, we get

$$\begin{aligned} I_{p\nu,q\nu'}(\boldsymbol{Q}) \approx {} & 8(-1)^{\nu'}(\nu'\nu)^{5/2} f_{qp}^{3/2}[(f_{qp}-1)(\nu^2-(\nu' f_{qp})^2) - (f_{qp}+1)Q'^2] \\ & \times \frac{[\nu^2-(\nu' f_{qp})^2-Q'^2]^{\nu'-1}[\nu^2-(\nu' f_{qp})^2+Q'^2]^{\nu-1}}{[(\nu-\nu' f_{qp})^2+Q'^2][(\nu+\nu' f_{qp})^2+Q'^2]} \\ & \times F\left[1-\nu', 1-\nu, 2, \frac{-4\nu'\nu f_{qp}}{(\nu-\nu' f_{qp})^2+Q'^2}\right]. \end{aligned} \tag{18}$$

Then, taking the limit $Q \to 0$, this expression reduces to equation (15) of [30] for the exciton transition between q- and p-bands via the DP exciton–phonon interaction, and for $f_{qp} \approx 1$ the expression reduces to equation (15) of [31] for exciton transitions between states of the same exciton via the F exciton–phonon interaction.

For the discrete–continuous transition the matrix element $I_{p\nu,q\nu'}(\boldsymbol{Q})$ is given by equation (17) of [31].

4. Selection rules

In order to carry out a more effective analysis of the different processes taking place in the multiphonon Raman scattering, it is necessary to obtain some selection rules, which allow the study of electronic states, phonons, and their interaction. Following the considerations above, it is possible to express the scattering process using the diagram given as figure 1, where the

allowed and forbidden transitions for different scattering configurations are clearly shown; a particular incident and emitted light polarization is considered.

The wavefunctions for conduction and valence bands, with $J = 3/2$ for Γ_8^v, and $J = 1/2$ for Γ_6^c and Γ_7^s, can be represented as [21]

$$c^+ = |\tfrac{1}{2}, +\tfrac{1}{2}\rangle = |S\uparrow\rangle, \qquad c^- = |\tfrac{1}{2}, -\tfrac{1}{2}\rangle = |S\downarrow\rangle, \tag{19}$$

$$v_{hh}^+ = \left|\frac{3}{2}, +\frac{3}{2}\right\rangle = \frac{1}{\sqrt{2}}|(X + \mathrm{i}Y)\uparrow\rangle, \qquad v_{hh}^- = \left|\frac{3}{2}, -\frac{3}{2}\right\rangle = \frac{1}{\sqrt{2}}|(X - \mathrm{i}Y)\downarrow\rangle, \tag{20}$$

$$v_{lh}^+ = \left|\frac{3}{2}, +\frac{1}{2}\right\rangle = \frac{1}{\sqrt{6}}|(X + \mathrm{i}Y)\downarrow - 2Z\uparrow\rangle, \qquad v_{lh}^- = \left|\frac{3}{2}, -\frac{1}{2}\right\rangle = \frac{1}{\sqrt{6}}|(X - \mathrm{i}Y)\uparrow + 2Z\downarrow\rangle, \tag{21}$$

$$v_{so}^+ = \left|\frac{1}{2}, +\frac{1}{2}\right\rangle = \frac{1}{\sqrt{3}}|(X + \mathrm{i}Y)\downarrow + Z\uparrow\rangle, \qquad v_{so}^- = \left|\frac{1}{2}, -\frac{1}{2}\right\rangle = \frac{1}{\sqrt{3}}|(X - \mathrm{i}Y)\uparrow - Z\downarrow\rangle, \tag{22}$$

where $\uparrow$ ($\downarrow$) denotes spin 'up' ('down') for the band wavefunction.

For circularly polarized light (Faraday configuration, $\boldsymbol{B} \parallel \boldsymbol{\kappa}_l \parallel \boldsymbol{z}$) the optical interband transitions allowed for incident light with the polarization vector

$$\hat{\boldsymbol{e}}_l = \hat{\boldsymbol{e}}_\pm = \frac{\hat{\boldsymbol{e}}_x \pm \mathrm{i}\hat{\boldsymbol{e}}_y}{\sqrt{2}} \tag{23}$$

are given by the matrix element $\langle c|\hat{\boldsymbol{e}}_l \cdot \hat{\boldsymbol{p}}_l|v\rangle \neq 0$. These allowed transitions are indicated by a solid line in figure 1. These selection rules allow only certain excitons to be excited, according to the polarization of the incident radiation. The different excitonic branches are very far apart in energy if the applied magnetic field is strong enough. In subsequent parts of this work we will keep in mind the results obtained in this section and will show how the scattering spectra change from one case to another.

Raman processes via DP exciton–phonon interaction are possible in the two scattering configurations $\bar{Z}(\hat{\boldsymbol{e}}_+, \hat{\boldsymbol{e}}_-)Z$ and $\bar{Z}(\hat{\boldsymbol{e}}_-, \hat{\boldsymbol{e}}_+)Z$, and the following selection rules are obtained [22]:

$$\Delta J_z = J_{zq} - J_{zp} = \pm 2 \tag{24}$$

(+2 for $\bar{Z}(\hat{\boldsymbol{e}}_-, \hat{\boldsymbol{e}}_+)Z$ and −2 for $\bar{Z}(\hat{\boldsymbol{e}}_+, \hat{\boldsymbol{e}}_-)Z$).

The coupling constant of the exciton–phonon interaction $G^{KK'}_{pv,qv'}(\boldsymbol{Q})$ is equal to zero if $v_q \neq v_p$ and $c_q \neq c_p$ in equation (7). From figure 1 we can observe that exciton transitions with $v_q = v_p$ and $c_q = c_p$ do not exist. We are only interested in the cases where $v_q = v_p$ with $c_q \neq c_p$ and $v_q \neq v_p$ with $c_q = c_p$. In figure 1 we can also observe that exciton transitions between excitonic bands with the same valence bands and different conduction bands for polarizations $\hat{\boldsymbol{e}}_+$ and $\hat{\boldsymbol{e}}_-$ in the Faraday configuration do not exist; therefore, only the transitions $T_{10,8}$, $T_{9,7}$, $T_{6,3}$, and $T_{5,2}$, which are mixed between polarizations $\hat{\boldsymbol{e}}_\pm$ and $\hat{\boldsymbol{\pi}}$, are possible. Thus, in the Faraday configuration the matrix element $\langle c_q|\delta\phi|c_p\rangle = 0$ if $c_q \neq c_p$.

We can also to observe in figure 1 that in the case when $v_q \neq v_p$ with $c_q = c_p$, the allowed transitions in the Faraday configuration for DP interactions are $T_{3,1}$, $T_{4,2}$, $T_{7,1}$, $T_{7,3}$, $T_{8,2}$, $T_{8,4}$; however, the transitions $T_{7,3}$ and $T_{8,2}$ are forbidden because $\Delta J_z = 0$ in these transitions. In the polarizations $\hat{\boldsymbol{\pi}}$ and $\hat{\boldsymbol{e}}_\pm$ mixed with $\hat{\boldsymbol{\pi}}$, the allowed transitions are $T_{10,7}$, $T_{10,5}$, $T_{10,3}$, $T_{10,1}$, $T_{9,8}$, $T_{9,6}$, $T_{9,4}$, $T_{9,2}$, and $T_{8,6}$.

Considering LO phonons interacting via DP interaction just in the Faraday configuration, we can introduce the following definition:

$$T_{p,q} = \langle v_q|\delta\phi_{DP}^{(LO)}|v_p\rangle = \hat{\boldsymbol{e}}_{LO} \cdot \langle v_q|\boldsymbol{u}_0 \frac{\partial V_{eff}}{\partial \boldsymbol{u}_{rel}}|v_p\rangle, \tag{25}$$

and using the Bloch functions corresponding to the valence bands given in equations ((20)–(22)), the only nonzero values for the exciton transitions $p \to q$ are

$$\begin{aligned} T_{3,1} &= -T_{1,3} = T_{4,2} = -T_{2,4} = \frac{\mathrm{i}}{2}\frac{u_0}{a_0}D_{opt} \\ T_{7,1} &= -T_{1,7} = T_{8,4} = -T_{4,8} = \frac{\mathrm{i}}{2}\frac{u_0}{a_0}D_{opt}\sqrt{2} \end{aligned} \tag{26}$$

where a_0 is the lattice constant and is D_{opt} the optical DP, which is given by

$$D_{opt} = \frac{2a_0}{\sqrt{3}}\langle X|\frac{\partial V_{eff}}{\partial u_z}|Y\rangle. \tag{27}$$

It has been demonstrated that the DP is important only in processes of first order with $Q \to 0$.

In the case of LO phonons interacting via F exciton–phonon interaction, the interband contributions are of second order and can be neglected in the calculation of the exciton distribution function; therefore, the only allowed excitonic transitions are those between different internal states of the same excitonic band. Thus, we can define

$$\begin{aligned} T_{p,q} &= \langle c_q|\delta\phi_F^{(LO)}|c_p\rangle = \frac{1}{\sqrt{V}}\frac{C_F}{Q}\hat{e}_{LO}\cdot\langle c_q|\boldsymbol{Q}|c_p\rangle = \frac{1}{\sqrt{V}}\frac{C_F}{Q}\delta_{c_q,c_p} \\ T_{p,q} &= \langle v_q|\delta\phi_F^{(LO)}|v_p\rangle = \frac{1}{\sqrt{V}}\frac{C_F}{Q}\hat{e}_{LO}\cdot\langle v_q|\boldsymbol{Q}|v_p\rangle = \frac{1}{\sqrt{V}}\frac{C_F}{Q}\delta_{v_q,v_p}. \end{aligned} \tag{28}$$

From these results we can conclude that the F exciton–phonon interaction is totally intraband, between the same q-exciton states, and it is only allowed in the $\bar{Z}(\hat{e}_+, \hat{e}_+)Z$ and $\bar{Z}(\hat{e}_-, \hat{e}_-)Z$ scattering configurations. In the same way, the DP exciton–phonon interaction is of interband nature, between q- and p-excitons, and it is only possible in the scattering configurations $\bar{Z}(\hat{e}_+, \hat{e}_-)Z$ and $\bar{Z}(\hat{e}_-, \hat{e}_+)Z$.

5. Theory of multiphonon resonant Raman scattering in diluted magnetic semiconductors

The purpose of this section is to clarify the different roles of hot exciton transitions and their main contribution to the N-process Raman scattering cross-section. These results will be applied in studying MPRRS processes in wide-gap DMS, where the excitonic transitions are mediated by F exciton–phonon interaction and DP exciton–phonon interaction, and where transitions between different types of exciton (q and p) in the different scattering configurations are possible.

5.1. The differential cross-section

The excitonic transitions of the DMS with the emission of a LO phonon, under resonance conditions, can be considered as real transitions. In this approximation, the different steps of a process of Nth order can be characterized by a $P(E)$ function of distribution of the exciton energy. Supposing the previous hypothesis to be valid, the MPRRS process cross-section for an indirectly created q-exciton can be written in the form [20]

$$\frac{\mathrm{d}^2\sigma_q}{\mathrm{d}\Omega\,\mathrm{d}\omega_s} = \frac{V_0^2\omega_s^2\eta(\omega_s)}{8\pi^3c^4\eta(\omega_l)}W_r(\omega_s), \tag{29}$$

where V_0 is the crystal volume, $\eta(\omega)$ is the refractive index of light, c is the velocity of light in the vacuum, and W_r is the probability per unit time, per unit solid angle, of the emission of a

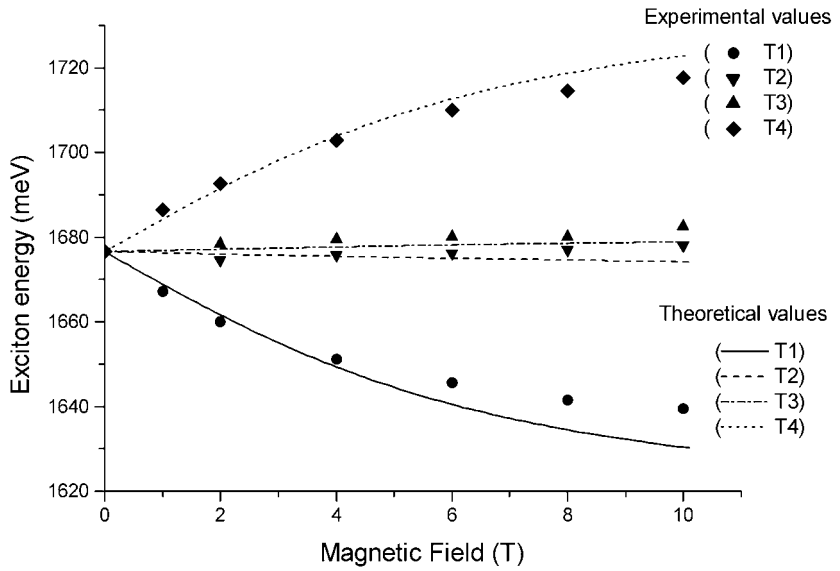

Figure 2. Exciton energies versus magnetic field magnitude B, at $\boldsymbol{k} = 0$, at $T = 5$ K and for Mn concentrations $x = 0.05$. The solid curves are the experimental results obtained from reflectivity data in $\hat{e}_+$- and $\hat{e}_-$-polarizations for T_1- and T_2-transitions (taken from [19]). The dashed curves are the corresponding theoretical results calculated from equation (32).

photon of frequency ω_s by a q- or p-exciton in the ν-state when a primary radiation quantum $\hbar\omega_l$ is absorbed by the crystal, creating a q-exciton in the ν-state. This probability is given by

$$W_r(\omega_s) = \sum_{\nu} \int P_{r\nu}(E) W^l_{r\nu}(E, \omega_s)\, \mathrm{d}E, \tag{30}$$

where r represents the q- or p-exciton if the cascade relaxation is intraband (F exciton–phonon interaction) or interband (DP exciton–phonon interaction), when the hot excitons are formed by indirect creation in the q-excitonic band, taking into account the light polarization and scattering configuration. ν represents the set of quantum numbers of the exciton, characterized by an energy $E_{q,\nu}(\boldsymbol{K})$ equal to

$$E_{q,\nu}(\boldsymbol{K}) = E_q(\boldsymbol{B}, T) - \Delta E_{q,\nu} + \frac{\hbar^2 K^2}{2m_{qT}}, \tag{31}$$

where $E_q(\boldsymbol{B}, T)$ is the effective energy gap corresponding to the q-exciton and is equal to

$$E_q(\boldsymbol{B}, T) = E_0 + \Delta_0 \delta_{J_h,1/2} + 2[3J_{ze}A_e(\boldsymbol{B}, T) - (-1)^{(2J_h+1)/2} J_{zh} A_h(\boldsymbol{B}, T)], \tag{32}$$

and $m_{qT} = m_e + m_{qh}$ is its total mass. For the discrete spectrum we obtain $\Delta E_{q,\nu} = R_q/n^2$ and for the continuum one $\Delta E_{q,k_{in}} = -R_q k^2 = -R_q(a_q k_{in})^2$, where R_q is the exciton Rydberg, a_q its Bohr radius, and $\boldsymbol{k}_{in} = (m_h \boldsymbol{k}_e - m_e \boldsymbol{k}_h)/m_T$ its internal wavevector. $P_{q\nu}(E)\,\mathrm{d}E$ is the number of excitons with energies within the interval $(E,\ E+\mathrm{d}E)$, and $W^l_{r\nu}(E, \omega_s)$ is the indirect annihilation probability, per unit time and per solid angle, due to simultaneous emission of an $\hbar\omega_0$ phonon and an $\hbar\omega_s$ photon for a q- or p-exciton in the internal state ν. n characterizes the internal state of the excitons (the main quantum number).

Figure 2 shows exciton energies obtained from reflectivity data as a function of the magnetic field [19]. Comparing these experimental results and equation (32) we can observe that the effect of the magnetic field, for moderate values, $B < 10$ T, can be considered as just as

a gap variation; i.e. the magnetic field intensity is not enough to produce Landau quantization. The Landé factors used to adjust the theoretical curve with the experimental data are 0.5 for electrons, 1.0 for heavy holes, and 0.5 for light holes.

We consider $Cd_{1-x}Mn_xTe$ as the ternary polar direct gap semiconductor below the Debye temperature where the exciting radiation frequency ω_l obeys the following condition:

$$\hbar\omega_l > E_q(\boldsymbol{B}, T) - \Delta E_{q,\nu} + N\hbar\omega_0; \qquad N = 2, 3, \ldots. \tag{33}$$

5.2. Hot exciton distribution function balance equations

From equation (30) we can see that in order to calculate the differential scattering cross-section we need to know the indirect creation probability and the $P_{r\nu}(E)$ distribution function for each excitonic branch present in the system. A simple estimate for $P_{r\nu}(E)$ can be obtained by proving the validity of the balance equation hypothesis. For an isotropic $P_{r\nu}(E)$ exciton distribution, in which there exist ten exciton bands, the Boltzmann equation is given by

$$\frac{\partial P_{r\nu}}{\partial t} = \sum_p \left\{ \sum_{\nu'} \int P_{p\nu'}(E') W_{p\nu'\to q\nu}(E', E)\,\mathrm{d}E' - \sum_{\nu'} \int P_{q\nu}(E) W_{q\nu\to p\nu'}(E, E')\,\mathrm{d}E' \right\} + W^{ex}_{q\nu}\delta(E - E_{on}) \tag{34}$$

where $W_{p\nu'\to q\nu}(E', E)\,\mathrm{d}E$ is the rate of transitions induced by phonon coupling between the p-exciton in the internal state ν' ($p = q$ with $\nu' \neq \nu$ is included (F exciton–phonon interaction)) and the q-exciton in the internal state ν ($\nu' = \nu$ is allowed for $p \neq q$ (DP exciton–phonon interaction)). $W^{ex}_{q\nu}$ is the indirect exciton creation probability for one of the ten excitons indicated in figure 1; we have taken into account the polarization of the light that illuminates the crystal. $E_{0n} = \hbar\omega_l - E_{q\nu}(\boldsymbol{B}, T) - \hbar\omega_0 + R_q/n^2$ is the initial kinetic energy of the exciton produced by the incident photon.

The first term on the right-hand side of equation (34) represents all the contributions per unit time due to the q-exciton in the ν-state, with kinetic energy E, and conversely for the second term.

In the stationary case, $\partial P_{r\nu}/\partial t = 0$, and it is clear that

$$\sum_p \sum_{\nu'} \int W_{q\nu\to p\nu'}(E, E')\,\mathrm{d}E' = \gamma_{q\nu}(E), \tag{35}$$

where $\gamma_{q\nu}(E)$ is the generalized exciton reciprocal lifetime, which includes all the excitonic contributions due to the same hot exciton and different types of exciton.

In DMS, when the exciton kinetic energy exceeds $\hbar\omega_0$, the transition probability $W_{q\nu\to p\nu'}(E, E')$ is basically determined by F exciton–LO phonon interaction (F) and DP exciton–LO and TO phonon interaction (DP). Then, $W_{q\nu\to p\nu'}(E, E')$ is given by

$$W_{q\nu\to p\nu'}(E, E') = W_{q\nu\to p\nu'}(E')\delta\left(E' - \frac{R_p}{n'^2} - E + \frac{R_q}{n^2} - \hbar\omega_0\right), \tag{36}$$

where $W_{q\nu\to p\nu'}(E')$ is the probability of transition per unit time for the p-exciton in the ν-state, with kinetic energy E, due to the emission of an $\hbar\omega_0$ phonon.

Using equations (35) and (36), equation (34) can be written as

$$P_{q\nu}(E)\gamma_{q\nu}(E) = \sum_p \sum_{\nu'} \int P_{p\nu'}(E') W_{p\nu'\to q\nu}(E') \times \delta\left(E' - \frac{R_p}{n'^2} - E + \frac{R_q}{n^2} - \hbar\omega_0\right)\mathrm{d}E' + W^{ex}_{q\nu}\delta(E - E_{on}). \tag{37}$$

This equation represents an inhomogeneous system of integral equations whose solution is found by successive iteration (see (16)). The general solution for the $(N+1)$-phonon process takes the following form:

$$P_{q\nu_N}(E) = \frac{\delta(E+(N-1)\hbar\omega_0 - E_{0n_N})}{\gamma_{q\nu_N}(E_{0n_N}-(N-1)\hbar\omega_0)} W^{ex}_{q\nu_1} \times \sum_p \left\{ \sum_{\nu_1,\ldots,\nu_{N-1}} \prod_{j=1}^{N-1} \left[\frac{W_{p\nu_j \to q\nu_{j+1}}(E_{0n_j}-(j-1)\hbar\omega_0)}{\gamma_{pn_j}(E_{0n_j}-(j-1)\hbar\omega_0)} \right] \right\} \tag{38}$$

with

$$E_{0n_N} - N\hbar\omega_0 < E < E_{0n_N} - (N-1)\hbar\omega_0. \tag{39}$$

The above expression contains all the possible contributions to the exciton distribution function for the q-exciton in any ν-state, with kinetic energy E. It has the necessary information for the $(N+1)$-phonon process in DMS if the relation $E_{0n_N} > (N-1)\hbar\omega_0$ is satisfied.

Using equations (29), (30), and (38), the differential scattering cross-section for an N-phonon process in the q-exciton band, with the participation of p-exciton bands, is given by

$$\frac{d^2\sigma_q^{N\omega_0}}{d\Omega\, d\omega_s} = \frac{V_0^2\omega_s^2\eta(\omega_s)}{(2\pi)^3c^4\eta(\omega_l)} W^{ex}_{q\nu_1} \sum_p \left\{ \sum_{\nu_1,\ldots,\nu_{N-1}} \prod_{j=1}^{N-2} \left[\frac{W_{p\nu_j \to q\nu_{j+1}}(E_{0n_j}-(j-1)\hbar\omega_0)}{\gamma_{pn_j}(E_{0n_j}-(j-1)\hbar\omega_0)} \right] \right\} \times \frac{W^l_{r\nu_{N-1}}(E_{0n_{N-1}}-(N-2)\hbar\omega_0,\omega_s)}{\gamma_{r\nu_{N-1}}(E_{0n_{N-1}}-(N-2)\hbar\omega_0,\omega_s)}. \tag{40}$$

The above expression contains all the information related to the cascade relaxation of the excitons in the q-band with the $N-1$ successively emitted phonons and a subsequent indirect annihilation with the emission of the last phonon in the DMS, if the condition $\hbar\omega_l - E_{q\nu}(\boldsymbol{B},T) + R_q/n^2 > N\hbar\omega_0$ is fulfilled.

If we do not take into account the selection rules for the light polarization vector, the general total differential cross-section for a MPRRS process in DMS is given by

$$\frac{d^2\sigma^{N\omega_0}}{d\Omega\, d\omega_s} = \sum_{q=1}^{10} \frac{d^2\sigma_q^{N\omega_0}}{d\Omega\, d\omega_s}. \tag{41}$$

6. The differential scattering cross-section in DMS

In DMS the hole effective mass is much greater than the electron effective mass, $m_h \gg m_e$; therefore, the indirect creation and annihilation of a hot q-exciton occurs in the 1s state [16]. We will also consider the approximation in which the wavevector of the DP phonons is zero, $Q_{DP} = 0$, and the Faraday configuration for the incident photon. Therefore, the hot excitons can only be indirectly created by F phonons and can be indirectly annihilated, via F phonons, or directly, via DP phonons. In our analysis we will only consider the following cases:

(i) First a hot q-exciton in the ground state $n = 1$, with quasi-momentum $\hbar\boldsymbol{k} \neq 0$, is indirectly created by absorption of a photon of energy $\hbar\omega_l$, taking into account the polarization of the light; an F phonon of frequency ω_{LO} is simultaneously emitted.

(ii) The hot q-exciton in the 1s state can undergo a cascade relaxation but staying in the same state, with the emission of F phonons, and we consider all the contributions of other p-excitons and other internal ν-states of the same q-exciton as the intermediate states. This cascade relaxation can only be performed in the $\bar{Z}(\hat{e}_+,\hat{e}_+)Z$ and $\bar{Z}(\hat{e}_-,\hat{e}_-)Z$ scattering configurations.

(iii) The q-exciton is indirectly created in the 1s state, emitting a F phonon, and then it makes transitions to other p-exciton states, emitting a DP phonon in each transition; we have to take into account the selection rules for the DF exciton phonon interaction. Finally, the exciton can be indirectly annihilated from the 1s state of the p-exciton band, emitting the last F phonon. The process is only possible in $\bar{Z}(\hat{e}_+, \hat{e}_-)Z$ and $\bar{Z}(\hat{e}_-, \hat{e}_+)Z$ scattering configurations.

(iv) The q-exciton of case (ii) carries out a complete cascade relaxation until the border of the band is reached, emitting an F phonon in each transition; then it makes transitions between the borders of the p-excitons emitting a DP phonon in each transition. Finally, it is directly annihilated. In this case all scattering configurations are possible.

(v) The q-exciton of case (iii) carries out a relaxation by interband transitions, emitting a DP phonon in each transition; then it undergoes a cascade relaxation in the p-exciton, emitting an F phonon in each transition. Finally, the p-exciton is annihilated. In this case all scattering configurations are possible.

There can be other combinations, but we will only consider these cases in our theory.

In case (ii) the general expression for the scattering differential cross-section can be obtained from equation (40), making $\nu = (1, 0, 0)$, $p = q, r = q, \omega_0 = \omega_{LO}^F$, and eliminating the sum in P; thus,

$$\frac{\mathrm{d}^2\sigma_q^{N\omega_0}}{\mathrm{d}\Omega\,\mathrm{d}\omega_s} = \frac{V_0^2\omega_s^2\eta(\omega_s)}{8\pi^3c^4\eta(\omega_l)}W^{ex}_{q(1,0,0)}\left\{\sum_{\nu_1,\ldots,\nu_{N-1}}\prod_{j=1}^{N-2}\left[\frac{W_{q\nu_j\to q\nu_{j+1}}(E_{0,1}-(j-1)\hbar\omega_{LO}^F)}{\gamma_q(E_{0,1}-(j-1)\hbar\omega_{LO}^F)}\right]\right\} \times \frac{W^l_{q(1,0,0)_{N-1}}(E_{0,1}-(N-2)\hbar\omega_{LO}^F,\omega_s)}{\gamma_{q(1,0,0)_{N-1}}(E_{0,1}-(N-2)\hbar\omega_{LO}^F,\omega_s)}. \tag{42}$$

In case (iii) the general expression for the scattering differential cross-section is obtained by making $\nu = (1, 0, 0)$, $p \neq q, r = p, \omega_0 = \omega_{LO}^{DP}$, and it is given by

$$\frac{\mathrm{d}^2\sigma_q^{N\omega_0}}{\mathrm{d}\Omega\,\mathrm{d}\omega_s} = \frac{V_0^2\omega_s^2\eta(\omega_s)}{8\pi^3c^4\eta(\omega_l)}W^{ex}_{q(1,0,0)}\sum_{p\neq q}\left\{\sum_{\nu_1,\ldots,\nu_{N-1}}\prod_{j=1}^{N-2}\left[\frac{W_{p\nu_j\to q\nu_{j+1}}(E_{0,1}-(j-1)\hbar\omega_{LO}^{DP})}{\gamma_p(E_{0,1}-(j-1)\hbar\omega_{LO}^{DP})}\right]\right\} \times \frac{W^l_{p(1,0,0)_{N-1}}(E_{0,1}-(N-2)\hbar\omega_{LO}^F,\omega_s)}{\gamma_{p(1,0,0)_{N-1}}(E_{0,1}-(N-2)\hbar\omega_{LO}^F,\omega_s)}. \tag{43}$$

In case (iv) it is necessary to add both contributions. However, in the latter equation the exciton can be directly annihilated by means of a DP exciton–phonon interaction; this is due to the exciton being at the border of the bands—it cannot be annihilated emitting an F phonon.

6.1. Scattering cross-sections for two and three phonons

The F phonons are the only contribution to the scattering cross-section for two phonons; in this case the hot exciton is indirectly created, emitting an F phonon, and then is also indirectly annihilated, emitting the second phonon (see figure 3(a)). The allowed scattering configuration for this case is $\bar{Z}(\hat{e}_\pm, \hat{e}_\pm)Z$, and the description is

$$\sigma^{2\hbar\omega_{LO}^F} = A\frac{V_0}{c'}W^{ex}_{q(1,0,0)}(E_{q0,1})\frac{W^l_{q(1,0,0)}(E_{q0,1}-\hbar\omega_{LO}^F)}{\gamma(E_{q0,1}-\hbar\omega_{LO}^F)}, \tag{44}$$

where c' is the speed of light in the crystal and A is a numerical factor depending on the ratio of the exciton reciprocal lifetime γ to the LO phonon reciprocal lifetime Y.

According to [23], $A = 2$ when $\gamma/Y \gg 1$, and $A = 1$ in the opposite case, $\gamma/Y \ll 1$. For our numerical calculations we have taken the second value.

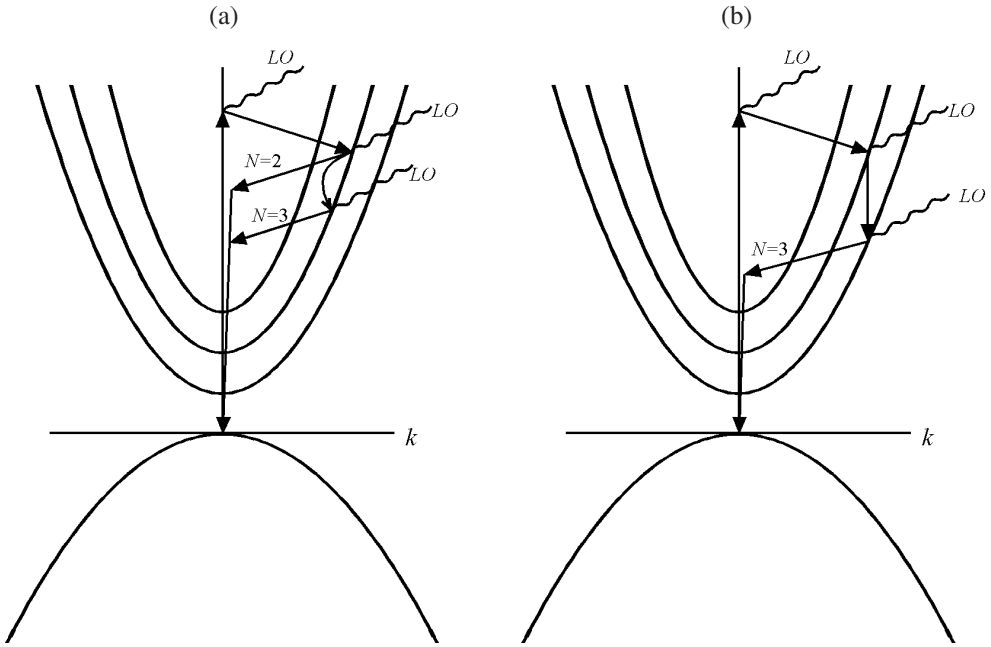

Figure 3. (a) A schematic representation of a process of second and third order, with the emission of two and three longitudinal optical phonons. The exciton–phonon interaction is considered to be of F type and only intraband transitions are allowed. (b) A schematic representation where, after the indirect creation of a q-exciton, emitting a F phonon, there is, due to the DP exciton–phonon interaction, an interband transition to p-exciton state; finally an indirect annihilation of the p-exciton occurs, emitting an F phonon.

As we said before, the contributions of different excitonic branches can be far apart, following the selection rules obtained previously. Thus, for a two-phonon process they are given as follows:

(a) Circular polarization of incident light, $\hat{e}_+$, with $\boldsymbol{B} \parallel \hat{z}$:

$$\sigma_{\hat{e}_+}^{2\hbar\omega_{LO}^F} = \sigma_1^{2\hbar\omega_{LO}^F} + \sigma_2^{2\hbar\omega_{LO}^F} + \sigma_8^{2\hbar\omega_{LO}^F}. \tag{45}$$

(b) Circular polarization of incident light, $\hat{e}_-$, with $\boldsymbol{B} \parallel \hat{z}$:

$$\sigma_{\hat{e}_-}^{2\hbar\omega_{LO}^F} = \sigma_3^{2\hbar\omega_{LO}^F} + \sigma_4^{2\hbar\omega_{LO}^F} + \sigma_7^{2\hbar\omega_{LO}^F}. \tag{46}$$

(c) Linear polarization of incident light, $\hat{\pi}$, $\boldsymbol{B} \parallel \hat{z}$:

$$\sigma_{\hat{\pi}}^{2\hbar\omega_{LO}^F} = \sigma_5^{2\hbar\omega_{LO}^F} + \sigma_6^{2\hbar\omega_{LO}^F} + \sigma_9^{2\hbar\omega_{LO}^F} + \sigma_{10}^{2\hbar\omega_{LO}^F}. \tag{47}$$

In the case of the scattering cross-section for three phonons, both F and DP phonons contribute. The hot exciton is indirectly created, emitting an F phonon, and then it makes an intraband transition via F hot exciton–phonon interaction (see figure 3(a)), or an interband transition via DP hot exciton–phonon interaction (see figure 3(b)). Finally, the exciton is indirectly annihilated, emitting the second F phonon (we only consider these cases). The allowed scattering configurations in this case are $\bar{Z}(\hat{e}_\pm, \hat{e}_\pm)Z$, for F interaction, and $\bar{Z}(\hat{e}_\pm, \hat{e}_\mp)Z$, for DP interaction. The corresponding expressions are

$$\sigma^{3\hbar\omega_{LO}^F} = A\frac{V_0}{c'}W^{ex}_{q(1,0,0)}(E_{q0,1})\frac{W_{s1}(E_{q0,1}-\hbar\omega_{LO}^F)}{\gamma(E_{q0,1}-\hbar\omega_{LO}^F)}\frac{W^l_{q(1,0,0)}(E_{q0,1}-2\hbar\omega_{LO}^F)}{\gamma(E_{q0,1}-2\hbar\omega_{LO}^F)} \tag{48}$$

for intraband transitions via F hot exciton–phonon interaction, and

$$\sigma^{2\hbar\omega^F_{LO}+\hbar\omega^{DP}_{LO}} = A\frac{V_0}{c'}W^{ex}_{q(1,0,0)}(E_{q0,1})\frac{W_{qp1}(E_{q0,1}-\hbar\omega^{DP}_{LO})}{\gamma(E_{q0,1}-\hbar\omega^{DP}_{LO})}\frac{W^l_{p(1,0,0)}(E_{q0,1}-\hbar\omega^F_{LO}-\hbar\omega^{DP}_{LO})}{\gamma(E_{q0,1}-\hbar\omega^F_{LO}-\hbar\omega^{DP}_{LO})} \tag{49}$$

for interband transitions via DP hot exciton–phonon interaction.

Taking into account the previous selection rules, the scattering configurations for three-phonon processes are $\bar{Z}(\hat{e}_\pm, \hat{e}_\pm)Z$; the corresponding expressions are as follows:

(a) Circular polarization of incident light, $\hat{e}_+$, with $\boldsymbol{B} \parallel \hat{z}$:

$$\sigma^{3\hbar\omega^F_{LO}}_{\hat{e}_+} = \sigma^{3\hbar\omega^F_{LO}}_1 + \sigma^{3\hbar\omega^F_{LO}}_2 + \sigma^{3\hbar\omega^F_{LO}}_8. \tag{50}$$

(b) Circular polarization of incident light, $\hat{e}_-$, with $\boldsymbol{B} \parallel \hat{z}$:

$$\sigma^{3\hbar\omega^F_{LO}}_{\hat{e}_-} = \sigma^{3\hbar\omega^F_{LO}}_3 + \sigma^{3\hbar\omega^F_{LO}}_4 + \sigma^{3\hbar\omega^F_{LO}}_7. \tag{51}$$

(c) Linear polarization of incident light, $\hat{\pi}$, $\boldsymbol{B} \parallel \hat{z}$:

$$\sigma^{3\hbar\omega^F_{LO}}_{\hat{\pi}} = \sigma^{3\hbar\omega^F_{LO}}_5 + \sigma^{3\hbar\omega^F_{LO}}_6 + \sigma^{3\hbar\omega^F_{LO}}_9 + \sigma^{3\hbar\omega^F_{LO}}_{10}. \tag{52}$$

If we only consider the Faraday configuration and the Stokes process for three-phonon MPRRS, we find that only the transitions $T_{1,3}$, $T_{2,4}$, and $T_{1,7}$ contribute for the scattering configuration $\bar{Z}(\hat{e}_+, \hat{e}_-)Z$. We also find that only the $T_{4,8}$-transition contributes to the $\bar{Z}(\hat{e}_-, \hat{e}_+)Z$ scattering configuration. To establish this we must take into account the selection rules for DP hot exciton–phonon interaction. These contributions are given by as follows:

(a) The scattering configuration $\bar{Z}(\hat{e}_+, \hat{e}_-)Z$:

$$\sigma^{2\hbar\omega^F_{LO}+\hbar\omega^{DP}_{LO}} = \sigma^{2\hbar\omega^F_{LO}+\hbar\omega^{DP}_{LO}}_{1,3} + \sigma^{2\hbar\omega^F_{LO}+\hbar\omega^{DP}_{LO}}_{2,4} + \sigma^{2\hbar\omega^F_{LO}+\hbar\omega^{DP}_{LO}}_{1,7}. \tag{53}$$

(b) The scattering configuration $\bar{Z}(\hat{e}_-, \hat{e}_+)Z$:

$$\sigma^{2\hbar\omega^F_{LO}+\hbar\omega^{DP}_{LO}} = \sigma^{2\hbar\omega^F_{LO}+\hbar\omega^{DP}_{LO}}_{4,8}. \tag{54}$$

In order to calculate the scattering cross-section by using equations (45)–(47) and (50)–(52), as well as its dependence on frequency and magnetic field, we need to know the total lifetime and transition probabilities of the hot exciton in a ν-state, with kinetic energy E, involved in the process. These magnitudes were already calculated, for $E > \hbar\omega_{LO}$, in [24–26]. There it was considered that transitions are mediated by an F phonon and that the width of the energy level E_n is equal to zero. In our numerical calculations we have generalized the earlier formulae to include some width of the energy level E_n and the magnetic field. In order to simplify the results, we do not consider the probabilities of transitions via DP exciton–phonon interaction.

6.2. The probability of indirect creation and annihilation of a hot exciton in the $\nu = 1$ state; Fröhlich interaction

The indirect creation of a q-exciton at the Γ point of the Brillouin zone, below the Debye temperature, has the following stages:

(a) absorption of a photon with energy $\hbar\omega_l$ and creation of an exciton in a state ν' with momentum $\hbar\boldsymbol{k} = 0$ (virtual state);
(b) exciton transition from the ν'-state to the state $\nu = 1$, with momentum $\hbar\boldsymbol{k} \neq 0$ (real state) and simultaneous emission of an F LO phonon with wavevector $\boldsymbol{Q} \approx -\boldsymbol{k}$.

The probability per unit time of this process is

$$W^{exc}_{q(1,0,0)} = \frac{2\pi}{\hbar}\sum_f \left| \sum_{\nu'} \frac{\langle f|\hat{H}_{exc-ph}|0,\nu'\rangle\langle\nu',0|\hat{H}_{e-l}|i\rangle}{E_i - E_{q\nu'} + \mathrm{i}\delta} \right|^2 \delta(E_f - E_i), \qquad (55)$$

where $E_i = \hbar\omega_l$, $E_f = \hbar\omega_{LO} + \hbar^2\boldsymbol{k}^2/(2m_{qT}) + E_{q\nu}$ and $\sum_{\nu'}$ denotes a sum over the complete set of discrete and continuous Wannier–Mott exciton states, with $E_{q\nu'}$ previously defined for the discrete and continuous spectra.

$\hat{H}_{e-l}$ is the electron–photon interaction operator. It has been shown [27] that the matrix element $\langle\nu',0|H_{e-1}|i\rangle$, for the allowed direct transition, can be expressed in a simple form in terms of the exciton wavefunction:

$$\langle\nu',0|H_{e-1}|i\rangle = -\frac{e}{m_0}\left(\frac{2\pi\hbar}{\omega_l\varepsilon_\infty}\right)^{1/2}\hat{\boldsymbol{e}}_l\cdot\hat{\boldsymbol{p}}_{cv}\psi_{\nu'}(0), \qquad (56)$$

where e and m_0 are the free electron charge and mass, respectively, ε_∞ is the high-frequency permittivity, $\hat{\boldsymbol{e}}_l$ is the photon polarization vector, $\hat{\boldsymbol{p}}_{cv}$ is the interband matrix element for the electron momentum, and $\psi_{\nu'}(\boldsymbol{r})$ is the wavefunction of the exciton internal state.

Then, the probability of exciton creation in the ground state $\nu = 1$, taking into account both contributions discrete and continuous spectra, is

$$\begin{aligned} W^{exc}_{q(1,0,0)}(Z_1) = {} & \frac{\sqrt{2}}{2}\sqrt{\frac{Z_1 - 1 + \sqrt{(Z_1-1)^2+\Gamma^2}}{(Z_1-1)^2+\Gamma^2}}\,\frac{\Gamma_q}{(Z_1 + \frac{E_{q_1}}{\hbar\omega_{LO}})}\left\{\left|\sum_{\nu'=1}^{4}\frac{2^5}{\nu'^3(Z_{\nu'} + \mathrm{i}\frac{\delta}{\hbar\omega_{LO}})}\right.\right. \\ & \times\left.\left(\frac{f_{\nu'}(y_2)}{\left[y_2 + (\frac{\nu'+1}{\nu'})^2\right]^{\nu'+1}} - \frac{f_{\nu'}(y_1)}{\left[y_1 + \left(\frac{\nu'+1}{\nu'}\right)^2\right]^{\nu'+1}}\right)\right|^2 \\ & + \left(\frac{\hbar\omega_{LO}}{\Delta E_q}\right)^2\left|\frac{N(y_2,t_0)}{D(y_2,t_0)} - \frac{N(y_1,t_0)}{D(y_1,t_0)}\right|^2 + 2\frac{\hbar\omega_{LO}}{\Delta E_q}\,\mathrm{Re}\left[\left|\sum_{\nu'=1}^{4}\frac{2^5}{\nu'^3(Z_{\nu'} + \mathrm{i}\frac{\delta}{\hbar\omega_{LO}})}\right.\right. \\ & \times\left.\left.\left(\frac{f_{\nu'}(y_2)}{\left[y_2 + (\frac{\nu'+1}{\nu'})^2\right]^{\nu'+1}} - \frac{f_{\nu'}(y_1)}{\left[y_1 + (\frac{\nu'+1}{\nu'})^2\right]^{\nu'+1}}\right)\right|\left(\frac{N(y_2,t_0)}{D(y_2,t_0)} - \frac{N(y_1,t_0)}{D(y_1,t_0)}\right)^*\right]\right\}. \end{aligned} \qquad (57)$$

The indirect annihilation of an exciton has the following stages:

(a) transition of the exciton from the ground state, with momentum $\hbar\boldsymbol{k} \neq 0$, to a ν'-state, with momentum $\hbar\boldsymbol{k} = 0$ (virtual or intermediate state), and simultaneous emission of a phonon with wavevector $\boldsymbol{Q} = \boldsymbol{k}$;

(b) direct annihilation of the exciton with emission of a photon of secondary radiation, with energy $\hbar\omega_s$.

The initial and final energies of system in this process are, respectively,

$$E_{q_i} = E_{q\nu}(\boldsymbol{B},T) - \frac{R_q}{\nu^2} + \frac{\hbar^2\boldsymbol{k}^2}{2m_{qT}} \qquad \text{and} \qquad E_f = \hbar\omega_{LO} + \hbar\omega_s; \qquad (58)$$

the energy of the intermediate state is $E_{q\nu'} = E_{q\nu} + \hbar\omega_{LO}$, where $E_{q\nu}$ has been previously defined in discussing the creation probability.

Considering the finite lifetime, the indirect annihilation probability is found to be

$$W^{l}_{q(1,0,0)}(Z) = \alpha_q \omega_{LO} \Lambda_q \frac{\left(Z + \frac{E_q}{\hbar\omega_{LO}} - 1\right)}{Z} \left\{ \left| \sum_{\nu=1}^{4} \frac{2^5}{\nu^3 (Z - 1 + \frac{\Delta E_q}{\hbar\omega_{LO}}(\frac{1}{\nu^2} - 1) + \mathrm{i}\frac{\delta}{\hbar\omega_{LO}})} \right.\right.$$
$$\times \left(\frac{f_\nu(x_2)}{[x_2 + (\frac{\nu+1}{\nu})^2]^{\nu+1}} - \frac{f_\nu(x_1)}{[x_1 + (\frac{\nu+1}{\nu})^2]^{\nu+1}} \right) \Bigg|^2$$
$$+ \left(\frac{\hbar\omega_{LO}}{\Delta E_q} \right)^2 \left| \frac{N(x_2,t)}{D(x_2,t)} - \frac{N(x_1,t)}{D(x_1,t)} \right|^2$$
$$+ 2\frac{\hbar\omega_{LO}}{\Delta E_q} \mathrm{Re} \left[\sum_{\nu=1}^{4} \frac{2^5}{\nu^3 (Z - 1 + \frac{\Delta E_q}{\hbar\omega_{LO}}(\frac{1}{\nu^2} - 1) + \mathrm{i}\frac{\delta}{\hbar\omega_{LO}})} \right.$$
$$\left.\left.\left. \times \left(\frac{f_\nu(x_2)}{[x_2 + (\frac{\nu+1}{\nu})^2]^{\nu+1}} - \frac{f_\nu(x_1)}{[x_1 + (\frac{\nu+1}{\nu})^2]^{\nu+1}} \right) \left(\frac{N(x_2,t)}{D(x_2,t)} - \frac{N(x_1,t)}{D(x_1,t)} \right)^* \right] \right\}. \quad (59)$$

In both expressions for probabilities the following appear:

$$f_1(y) = 1, \qquad f_2(y) = y, \qquad f_3(y) = y^2 + \tfrac{1}{3}(\tfrac{4}{3})^2 y, \qquad f_4(y) = y^3 + \tfrac{11}{8}y^2 + \tfrac{1}{4}(\tfrac{5}{4})^3 y,$$

$$E_{q\nu} = E_q(\boldsymbol{B}, T) - \frac{\Delta E_q}{\nu^2}, \qquad Z_0 = \frac{\hbar\omega_l - E_q(\boldsymbol{B}, T)}{\hbar\omega_{LO}}, \qquad Z_\nu = \frac{\hbar\omega_l - E_{q\nu}}{\hbar\omega_{LO}},$$

$$Z = \frac{\frac{\hbar^2 k^2}{2m_{q\nu}}}{\hbar\omega_{LO}} = \frac{\hbar\omega_l - E_{q1} - \hbar\omega_{LO} + \Delta E_i}{\hbar\omega_{LO}},$$

$$t_0 = \frac{\hbar\omega_{LO}}{\Delta E_q} Z_0, \qquad t = \frac{\hbar\omega_{LO}(Z-1)}{\Delta E_q} - 1,$$

$$y_1 = \frac{\hbar\omega_{LO}}{\Delta E_q} \frac{m_e}{m_{qh}} (Z_1 - 1), \qquad y_2 = \frac{\hbar\omega_{LO}}{\Delta E_q} \frac{m_{qh}}{m_e} (Z_1 - 1),$$

$$x_2 = \frac{m_{qh}\hbar\omega_{LO}}{m_e \Delta E_q} Z, \qquad x_1 = \frac{m_e \hbar\omega_{LO}}{m_{qh} \Delta E_q} Z,$$

$$\Gamma_q = 4\alpha_q \omega_{LO} \left(\frac{\Delta E_q}{\hbar\omega_{LO}} \right)^2 \frac{\varepsilon_0 \mu_q}{\varepsilon_\infty m_0^2} \frac{|\hat{\boldsymbol{e}}_l \cdot \hat{\boldsymbol{p}}_{cv}|^2}{\hbar\omega_{LO}},$$

$$\Lambda_q = 2^{1/2} \varepsilon_0 \varepsilon_\infty^{1/2} \left(\frac{\Delta E}{m_0} \right)^2 \mu_q \frac{|\hat{\boldsymbol{e}}_s \cdot \hat{\boldsymbol{p}}_{cv}|^2}{(\hbar\omega_{LO} m_{qT} c^2)^{3/2}},$$

$$\alpha_q = \frac{e^2}{2\hbar\omega_{LO} l_q} (\varepsilon_\infty^{-1} - \varepsilon_0^{-1}), \qquad l_q = \left(\frac{\hbar}{2 m_{qT} \omega_{LO}} \right)^{1/2},$$

$$\mu_q = \frac{m_e m_{qh}}{m_{qT}}, \qquad m_{qT} = m_e + m_{qh},$$

as well as the following functions:

$$D(y,t) = \left[W_1^2(y,t) - 16 \left(\frac{\delta}{\Delta E} \right)^2 y \right] y,$$

$$N(y,t) = 4y \sqrt{\left| t + \mathrm{i}\frac{\delta}{\Delta E} \right|} \left[W_2(y,t) \cos\frac{\theta}{2} + \Delta_2(y,t) \sin\frac{\theta}{2} \right]$$

$$+\frac{2\delta}{\Delta E}\sqrt{y(y+1)}\left\{[W_1(y,t)-8y]\cos\frac{\varphi}{2}-\Delta_1(y,t)\sin\frac{\varphi}{2}\right\}$$
$$+\mathrm{i}\left\{4y\sqrt{\left|t+\mathrm{i}\frac{\delta}{\Delta E}\right|}\left(W_2(y,t)\cos\frac{\theta}{2}-\Delta_2(y,t)\sin\frac{\theta}{2}\right)\right.$$
$$+2\sqrt{y(y+1)}\left[(1-W_-(y,t))W_1(y,t)\cos\frac{\varphi}{2}\right.$$
$$\left.\left.+\sqrt{y}\left(4\left(\frac{\delta}{\Delta E}\right)^2-2W_1(y,t)\sin\frac{\varphi}{2}\right)\right]\right\},$$

where

$$W_1(y,t)=W_-^2(y,t)+2W_+(y,t)+\left(\frac{\delta}{\Delta E}\right)^2+1,$$
$$W_2(y,t)=(1-W_-(y,t))^2+4y-\left(\frac{\delta}{\Delta E}\right)^2,$$
$$\Delta_1(y,t)=4(1-W_-(y,t))\sqrt{y},$$
$$\Delta_2(y,t)=2(1-W_-(y,t))\frac{\delta}{\Delta E},\qquad W_\mp(y,t)=y\mp t,$$
$$\theta=\tan^{-1}\frac{\delta}{t\,\Delta E},$$
$$\varphi=\begin{cases}\tan^{-1}\dfrac{2\sqrt{y}}{y-1} & \text{if } y>1,\\ \pi+\tan^{-1}\dfrac{2\sqrt{y}}{y-1} & \text{if } y<1,\\ \dfrac{\pi}{2} & \text{if } y=1.\end{cases}$$

Figures 4 and 5 show the probabilities of exciton creation and annihilation, respectively, as functions of the incident radiation $\hbar\omega_l$ for several values of the magnetic field B. The calculations were based on the CdTe parameters [15]:

$$E_0=1.607\ \text{eV},\qquad \bar{a}=60\ \text{Å},$$
$$R_y=10.5\ \text{meV},\qquad Q=6\times10^{-3}\ \text{Å}^{-1},$$
$$\Delta_0=0.95\ \text{eV},\qquad m_e=0.09\,m_0,$$
$$\hbar\omega_{LO}=21\ \text{meV},\qquad m_{lh}=0.13\,m_0,$$
$$m_{hh}=0.72\,m_0,\qquad m_{so}=0.26\,m_0,$$

and the $Cd_{0.8}Mn_{0.2}Te$ parameters [15].

6.3. The lifetime of the hot excitons in the quantum state $\nu=1$

The total reciprocal lifetime for the q-exciton in the ground state $\nu=1$, with kinetic energy E, is defined as

$$\gamma(E)=W_s(E)+W_d(E)+\sum_{\nu\geqslant2}^{\infty}W^{(\nu)}(E),\tag{60}$$

where $W^{(\nu)}(E)$ is the probability of scattering of a q-exciton, accompanied by a transition from the $\nu=1$ (ground) state to a $\nu\geqslant2$ (excited) state belonging to the discrete internal energy spectrum of the same exciton. The expression for $\sum_{\nu\geqslant2}^{\infty}W^{(\nu)}(E)$ is given in [28] where the F

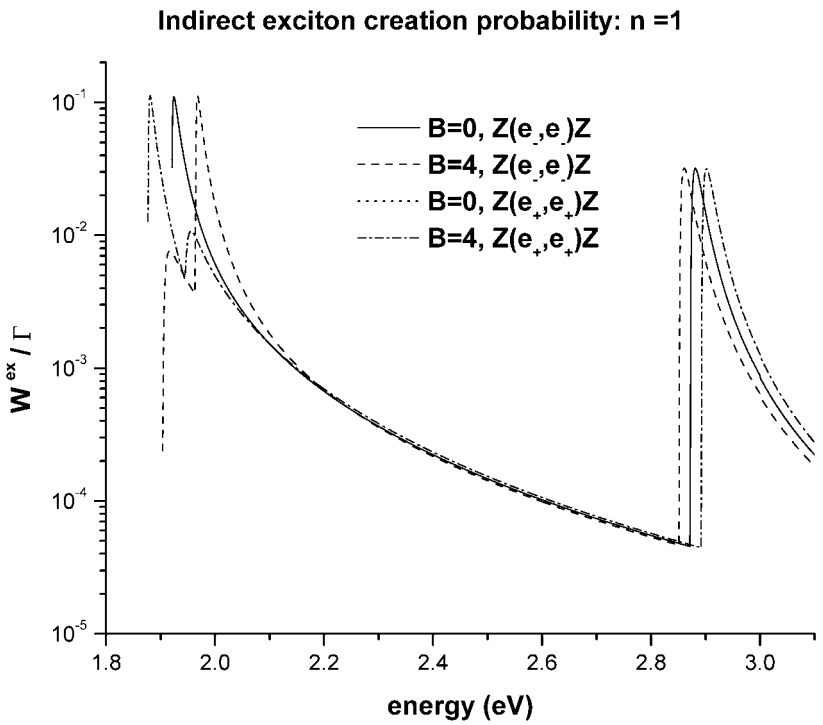

Figure 4. The dimensionless probability $W^{ex}_{q(1,0,0)}/\Gamma_q$ of exciton indirect creation as a function of the energy for the $\hat{e}_+$- and $\hat{e}_-$-polarizations and two values of the magnetic field B.

Hamiltonian in first order of perturbation theory was used. However, we have only considered the term with $\nu = 2$ in the sum because that term contributes more than others to the transition probabilities between $\nu = 1$ and $\nu \geqslant 2$ states. $W_d(E)$ is the probability of exciton decay with emission of one LO phonon. A general expression for this probability is given in [26], where the authors used a wavefunction corresponding to the continuous energy spectrum of the hydrogen atom to describe the final state; however, in the present work we have used a wavefunction for the continuous spectrum corresponding to a plane wave. W_s is the intraband transition probability for the same $\nu = 1$ internal state; i.e., there is no change in the exciton internal state.

Now we present compact expressions for these probabilities used in the calculations of the lifetime in this work [26, 28].

The intraband scattering probability W_s in the $\nu = 1$ state is given by

$$W_s(Z) = \frac{\alpha_q \omega_{LO}}{2\sqrt{Z}}[\Phi_\beta(\lambda_2) - \Phi_\beta(\lambda_1)], \tag{61}$$

with

$$\Phi_\beta(\lambda) = \left[\frac{2(1-3\beta)}{(1-\beta)^3} - 1\right] \ln\frac{1+\lambda}{1+\beta\lambda} + \left[1 - \frac{2}{(1-\beta)^2}\right]\frac{1}{1+\lambda} + \left[1 - \frac{2\beta^2}{(1-\beta)^2}\right] \times \frac{1}{1+\beta\lambda} + \frac{1}{2}\left[\frac{1}{(1+\lambda)^2} + \frac{1}{(1+\beta\lambda)^2}\right] + \frac{1}{3}\left[\frac{1}{(1+\lambda)^3} + \frac{1}{(1+\beta\lambda)^3}\right],$$

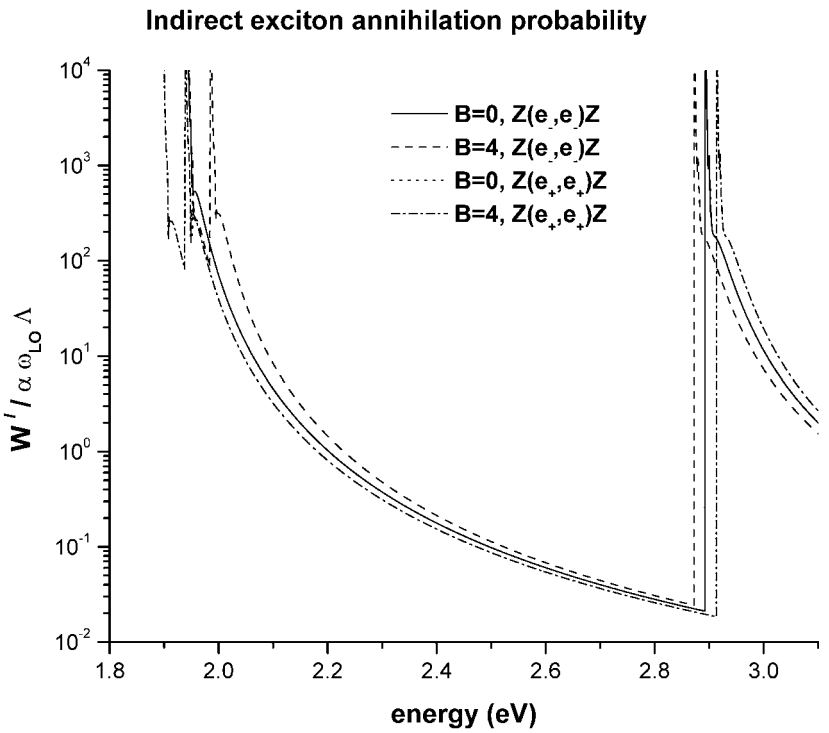

Figure 5. The dimensionless probability $W^{l}_{q(1,0,0)}/\alpha_q \omega_{LO} \Lambda_q$ of the exciton indirect annihilation as a function of the energy for the $\hat{e}_+$- and $\hat{e}_-$-polarizations and two values of the magnetic field B.

where

$$\lambda_{1,2} = \frac{1}{4\sqrt{\beta}} \frac{\hbar\omega_{LO}}{\Delta E_q} \left(\sqrt{Z} \mp \sqrt{Z-1}\right)^2, \qquad \beta = \left(\frac{m_{qh}}{m_e}\right)^2.$$

The probability $W^{(\nu)}$ of interband scattering for a q-exciton between $\nu = 1$ and 2 states is given by

$$W^{(1\to 2)}(Z) = -\frac{\alpha_q \omega_{LO}}{2^4\sqrt{Z}} [R(t_2) - R(t_1)], \tag{62}$$

with

$$R(t) = \frac{1}{4A^4} + \frac{1}{4B^4} + \frac{1}{\sqrt{\beta}-1}\frac{1}{(AB)^2} + \frac{32}{9}\frac{1}{(\sqrt{\beta}-1)^2} \times \left\{ -\frac{1}{A^2 B} + \frac{8}{3}\frac{1}{1-\beta}\left[\frac{1}{A^2} + \frac{32}{9}\frac{\beta}{\beta-1}\left(\frac{1}{A} + \frac{16}{9}\frac{\beta}{\beta-1}\ln\frac{B}{A}\right)\right]\right\}$$

and

$$A = t + \tfrac{9}{16}, \qquad B = \beta t + \tfrac{9}{16},$$

$$t_{1\to 2} = \frac{1}{4\sqrt{\beta}} \frac{\hbar\omega_{LO}}{\Delta E_q} \left[\sqrt{Z} \mp \sqrt{Z + \frac{\Delta E_q}{\hbar\omega_{LO}}\left(\frac{1}{2^2} - 1\right) - 1}\right]^2.$$

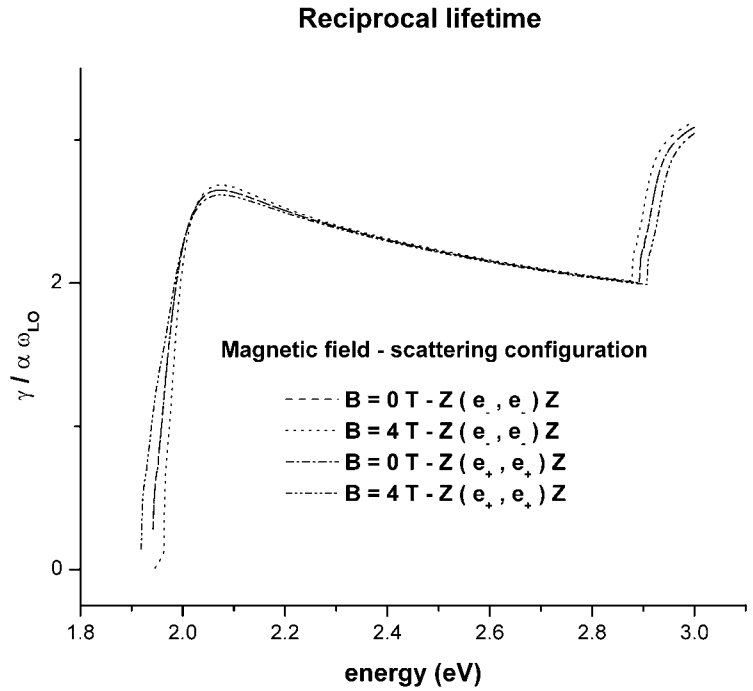

Figure 6. The dimensionless lifetime $\gamma/\alpha_q\omega_{LO}$ of the exciton as a function of the energy for the $\hat{e}_+$- and $\hat{e}_-$-polarizations and two values of the magnetic field B.

The decay probability W_d is calculated as the rate of disintegration of q-excitons in the $\nu = 1$ state to the continuous energy spectrum, and is given by the following expression:

$$W_d(Z) = \alpha_q\omega_{LO}\frac{2^4}{\pi\sqrt{Z}}\int_{\lambda_1}^{\lambda_2}\frac{\mathrm{d}q}{q}\int_0^{\delta(Q)}P^2\,\mathrm{d}P \times\int_{-1}^{1}\left\{\frac{1}{(\beta Q^2+P^2+2\sqrt{\beta}PQr+1)^2}-\frac{1}{(\beta Q^2+p^2-2\sqrt{\beta}pQr+1)^2}\right\}\mathrm{d}r, \tag{63}$$

with

$$\lambda_{1,2} = \beta^{-1/4}\left(\frac{\hbar\omega_{LO}}{\Delta E_q}\right)^{1/2}\left[\sqrt{Z}\mp\sqrt{Z-\frac{\Delta E_q}{\hbar\omega_{LO}}-1}\right],$$
$$\delta(Q) = \sqrt{\beta^{1/2}(Q-\lambda_1)(\lambda_2-Q)}.$$

In figure 6 we have shown the reciprocal lifetime as a function of the incident energy $\hbar\omega_l$ for several values of the magnetic field B.

In order to calculate the cross-section for scattering of two or three phonons via F exciton–phonon interaction, it is convenient to represent the indirect creation and annihilation probabilities and the lifetime in forms that allow one to simplify equations (57) and (59), taking into account the different excitons contributing (see figure 1). Thus, we obtain the following compact expressions:

$$W^{ex}_{q(1,0,0)}(Z_1) = \Gamma_q W^{ex}_q(Z+1), \qquad W^{l}_{q(1,0,0)}(Z) = \alpha_q\omega_{LO}\Lambda_q W^{l}_q(Z),$$
$$\gamma(Z) = \alpha_q\omega_{LO}\gamma_q(Z), \tag{64}$$

taking into account that

$$\Gamma_q \Lambda_q = 8e^2\mu_q^2 \left(\frac{\Delta E_q}{m_0}\right)^4 \frac{\varepsilon_0}{\varepsilon_\infty^{3/2}} \frac{1}{\hbar^6 \omega_{LO} m_{qT} c^3} |\hat{\boldsymbol{e}}_l \cdot \hat{\boldsymbol{p}}_{cv} \times \hat{\boldsymbol{e}}_s \cdot \hat{\boldsymbol{p}}_{cv}|_q^2$$

and defining

$$P_{p,q} = \frac{|\hat{\boldsymbol{e}}_l \cdot \hat{\boldsymbol{p}}_{cv} \times \hat{\boldsymbol{e}}_s \cdot \hat{\boldsymbol{p}}_{cv}|_p^2}{|\hat{\boldsymbol{e}}_l \cdot \hat{\boldsymbol{p}}_{cv} \times \hat{\boldsymbol{e}}_s \cdot \hat{\boldsymbol{p}}_{cv}|_q^2}.$$

Finally, the expressions used for the scattering cross-sections for two and three phonons, given by equations (64), are as follows:

(a) Circular polarization of incident light, $\hat{\boldsymbol{e}}_+$, with $\boldsymbol{B} \parallel \hat{\boldsymbol{z}}$:

$$\begin{aligned}
\sigma_{\hat{e}_+}^{2\hbar\omega_{LO}^F} = A\frac{V_0}{c}\Bigg\{ & W_1^{ex}(Z)\frac{W_1^l(Z-1)}{\gamma_1(Z-1)} + \frac{m_{1T}}{m_{2T}}\left(\frac{\mu_2}{\mu_1}\right)^6 P_{2,1} W_2^{ex}(Z)\frac{W_2^l(Z-1)}{\gamma_2(Z-1)} \\
& + \frac{m_{1T}}{m_{8T}}\left(\frac{\mu_8}{\mu_1}\right)^6 P_{8,1} W_8^{ex}(Z)\frac{W_8^l(Z-1)}{\gamma_8(Z-1)}\Bigg\}\Gamma_1\Lambda_1, \\
\sigma_{\hat{e}_+}^{3\hbar\omega_{LO}^F} = A\frac{V_0}{c}\Bigg[& W_1^{ex}(Z)\frac{W_{1s}(Z-1)}{\gamma_1(Z-1)}\frac{W_1^l(Z-2)}{\gamma_1(Z-2)} \\
& + \frac{m_{1T}}{m_{2T}}\left(\frac{\mu_2}{\mu_1}\right)^6 P_{2,1} W_2^{ex}(Z)\frac{W_{2s}(Z-1)}{\gamma_2(Z-1)}\frac{W_2^l(Z-2)}{\gamma_2(Z-2)} \\
& + \frac{m_{1T}}{m_{8T}}\left(\frac{\mu_8}{\mu_1}\right)^6 P_{8,1} W_8^{ex}(Z)\frac{W_{8s}(Z-1)}{\gamma_8(Z-1)}\frac{W_8^l(Z-2)}{\gamma_8(Z-2)}\Bigg]\Gamma_1\Lambda_1.
\end{aligned}$$

(b) Circular polarization of incident light, $\hat{\boldsymbol{e}}_-$, with $\boldsymbol{B} \parallel \hat{\boldsymbol{z}}$:

$$\begin{aligned}
\sigma_{\hat{e}_-}^{2\hbar\omega_{LO}^F} = A\frac{V_0}{c}\Bigg[& \frac{m_{1T}}{m_{3T}}\left(\frac{\mu_3}{\mu_1}\right)^6 P_{3,1} W_3^{ex}(Z)\frac{W_3^l(Z-1)}{\gamma_3(Z-1)} \\
& + \frac{m_{1T}}{m_{4T}}\left(\frac{\mu_4}{\mu_1}\right)^6 P_{4,1} W_4^{ex}(Z)\frac{W_4^l(Z-1)}{\gamma_4(Z-1)} \\
& + \frac{m_{1T}}{m_{7T}}\left(\frac{\mu_7}{\mu_1}\right)^6 P_{7,1} W_7^{ex}(Z)\frac{W_7^l(Z-1)}{\gamma_7(Z-1)}\Bigg]\Gamma_1\Lambda_1, \\
\sigma_{\hat{e}_-}^{3\hbar\omega_{LO}^F} = A\frac{V_0}{c}\Bigg[& \frac{m_{1T}}{m_{3T}}\left(\frac{\mu_3}{\mu_1}\right)^6 P_{3,1} W_3^{ex}(Z)\frac{W_{3s}(Z-1)}{\gamma_3(Z-1)}\frac{W_3^l(Z-2)}{\gamma_3(Z-2)} \\
& + \frac{m_{1T}}{m_{4T}}\left(\frac{\mu_4}{\mu_1}\right)^6 P_{4,1} W_4^{ex}(Z)\frac{W_{4s}(Z-1)}{\gamma_4(Z-1)}\frac{W_4^l(Z-2)}{\gamma_4(Z-2)} \\
& + \frac{m_{1T}}{m_{7T}}\left(\frac{\mu_7}{\mu_1}\right)^6 P_{7,1} W_7^{ex}(Z)\frac{W_{7s}(Z-1)}{\gamma_7(Z-1)}\frac{W_7^l(Z-2)}{\gamma_7(Z-2)}\Bigg]\Gamma_1\Lambda_1.
\end{aligned}$$

In a similar way, we can obtain the expression for the linear polarization of light, $\hat{\boldsymbol{\pi}}$, $\boldsymbol{B} \parallel \hat{\boldsymbol{z}}$.

7. Discussion of the results

In the calculations the following values of the parameters were used:

$$\begin{aligned}
&E_0 = 1.910\,\text{eV}, && \Delta_0 = 0.95\,\text{eV}, \\
&\hbar\omega_{LO} = 21\,\text{meV}, && C_F = 2.76 \times 10^{-5}\,\text{eV cm}^{1/2}, \\
&m_e = 0.09\,m_0, && m_{lh} = 0.13\,m_0,
\end{aligned}$$

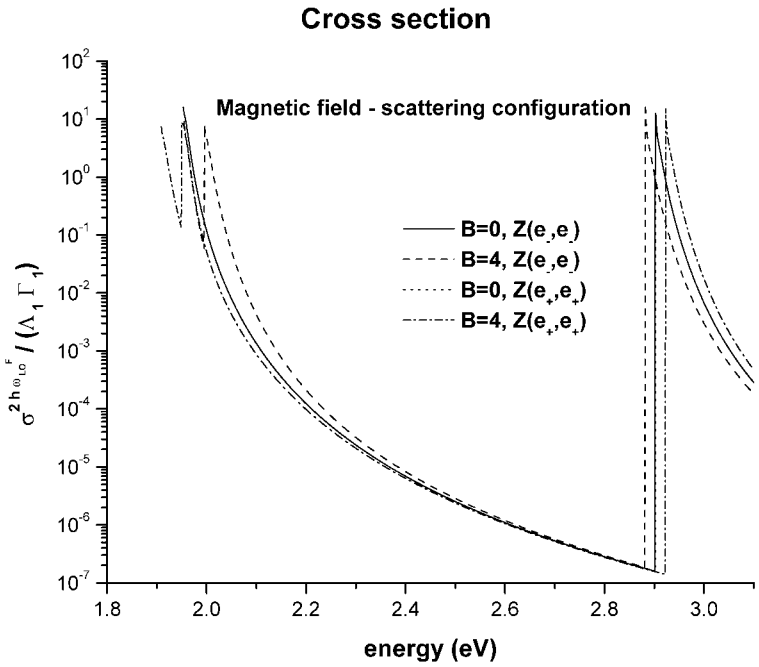

Figure 7. The second-order Raman intensity of the exciton as a function of the incident radiation energy $\hbar\omega_l$ for $\bar{Z}(\hat{e}_+, \hat{e}_+)Z$ and $\bar{Z}(\hat{e}_-, \hat{e}_-)Z$ scattering configurations with $B = 0$ and 4 T.

$$m_{hh} = 0.72\, m_0, \qquad m_{so} = 0.26\, m_0, \qquad T = 2\ \text{K},$$
$$N_0\alpha = 0.22\ \text{eV}, \qquad N_0\beta = -0.88\ \text{eV}, \qquad S_0 = 0.7, \qquad T_0 = 7.3\ \text{K}.$$

The data were taken from [15].

In figures 4–8 the exciton indirect creation probability (W^{ex}/Γ), the exciton indirect annihilation probability (W^{l}/Γ), the exciton reciprocal lifetime, and second- and third-order cross-sections are shown, as functions of the incident energy $\hbar\omega_l$, for two magnetic field values (0 and 4 T) and two scattering configurations: $\bar{Z}(\hat{e}_+, \hat{e}_+)Z$ and $\bar{Z}(\hat{e}_-, \hat{e}_-)Z$. In all cases, the behaviour of each of the excitons as displayed by the various curves can be determined by the ratio, as it is explained in [24, 26] and [28]; the ratio m_h/m_e remains the same. Thus, we focus our attention on the influence of the magnetic field on the magnitudes cited below.

In order to obtain each of the figures, the following values were used: $\delta_{T1} = 0.04\,\hbar\omega_{LO}$, $\delta_{T2} = \delta_{T3} = 0.05\,\hbar\omega_{LO}$, $\delta_{T4} = 0.07\,\hbar\omega_{LO}$, $\delta_{T7} = \delta_{T8} = 0.09\,\hbar\omega_{LO}$, $\Gamma_{T1} = 0.23$, $\Gamma_{T2} = \Gamma_{T3} = 0.28$, $\Gamma_{T4} = 0.33$, $\Gamma_{T7} = \Gamma_{T8} = 0.57$. On the other hand, the following relations were used too: $P_{2,1} = P_{3,1} = 1/9$, $P_{7,1} = P_{8,1} = 4/9$, $P_{4,1} = 1$.

In figure 4, the curves for $B = 0$ T and the scattering configurations $\bar{Z}(\hat{e}_+, \hat{e}_+)Z$ and $\bar{Z}(\hat{e}_-, \hat{e}_-)Z$ have maxima at the energy points $\hbar\omega_l = 1.925$, 2.881 eV; for $B = 4$ T and $\bar{Z}(\hat{e}_+, \hat{e}_+)Z$, at $\hbar\omega_l = 1.881$, 1.956, 2.902 eV; for $B = 4$ T and $\bar{Z}(\hat{e}_-, \hat{e}_-)Z$, at $\hbar\omega_l = 1.917$, 1.968, 2.861 eV. For $B = 4$ T the maxima corresponding to the energies $\hbar\omega_l = 1.881$ and 1.968 eV relate to heavy-exciton contributions, $\hbar\omega_l = 1.917$ and 1.956 eV to the light excitons, and $\hbar\omega_l = 2.861$ and 2.902 eV to the split-off excitons. The difference between the intensities of the exciton contributions can be understood through the ratio of effective masses m_h/m_e and the lifetime broadenings resulting from them.

The effect of the magnetic field is to move the maxima of the curves with respect to the $B = 0$ T cases in both scattering configurations. On the other hand, it can be observed

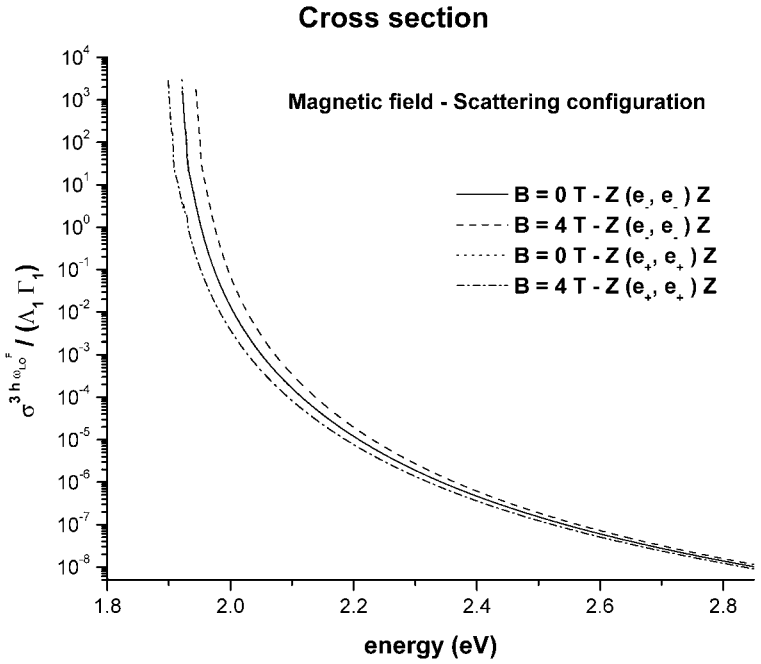

Figure 8. The third-order Raman intensity of the exciton as a function of the incident radiation energy $\hbar\omega_l$ for $\bar{Z}(\hat{e}_+, \hat{e}_+)Z$ and $\bar{Z}(\hat{e}_-, \hat{e}_-)Z$ scattering configurations with $B = 0$ and 4 T.

that the maxima positions depend on the scattering configuration selected. The energy difference between the maxima for the same type of exciton and relating to different scattering configurations is proportional to B. Thus, it is possible to find the Landé g-factor for each type of exciton.

In figure 5 the curves corresponding to $B = 4$ T and the $\bar{Z}(\hat{e}_+, \hat{e}_+)Z$ scattering configuration have maxima values for $\hbar\omega_l = 1.908$, 1.939, and 2.914 eV; for $B = 4$ T and $\bar{Z}(\hat{e}_-, \hat{e}_-)Z$, at $\hbar\omega_l = 1.945$, 1.985 and 2.873 eV; for $B = 0$ T and both scattering configurations, at $\hbar\omega_l = 1.942$ and 2.894 eV. The values $\hbar\omega_l = 1.908$ and 1.985 eV correspond to heavy-exciton contributions, $\hbar\omega_l = 1.939$ and 1.945 eV to light excitons, $\hbar\omega_l = 2.873$ and 2.914 eV to split-off excitons.

In the annihilation case, the magnetic field causes the displacements of the points of maxima values with respect to the $B = 0$ T case and the scattering configuration. The difference shown can also be explained by the difference in the ratios of the effective masses m_h/m_e and the lifetime broadenings for each exciton.

In figure 6 the reciprocal lifetimes ($\gamma/\alpha\omega_{LO}$) are presented as a function of the incident energy $\hbar\omega_l$. Similar behaviours for both curves for the reciprocal lifetime are observed for the two scattering configurations in the $B = 0$ T case. This is explained through the relation of the effective masses of holes and electrons m_h/m_e. However, the magnetic field produces a displacement of the positions of the maxima corresponding to $\bar{Z}(\hat{e}_+, \hat{e}_+)Z$ and $\bar{Z}(\hat{e}_-, \hat{e}_-)Z$ scattering configurations and changes of the $\gamma/\alpha\omega_{LO}$ values: for $\bar{Z}(\hat{e}_+, \hat{e}_+)Z$ the value is 2.61, while for $\bar{Z}(\hat{e}_-, \hat{e}_-)Z$ the value is 2.68.

In figure 7 it can be observed that the curves corresponding to the $\bar{Z}(\hat{e}_+, \hat{e}_+)Z$ and $\bar{Z}(\hat{e}_-, \hat{e}_-)Z$ configurations are the same for $B = 0$ T. As before, when the magnetic field is applied, displacements of the positions of the maxima corresponding to $\sigma/\Lambda_1\Gamma_1$ are produced.

In the scattering configuration $\bar{Z}(\hat{e}_+, \hat{e}_+)Z$, the values are $\hbar\omega_l = 1.953$ eV for $B = 0$ T and $\hbar\omega_l = 1.909$ and 1.950 eV for $B = 4$ T; in the $\bar{Z}(\hat{e}_-, \hat{e}_-)Z$ configuration, $\hbar\omega_l = 1.953$ eV for $B = 0$ T and $\hbar\omega_l = 1.955$ and 1.996 eV for $B = 4$ T. It can be observed that the positions of the maxima are quasi-symmetric with respect to the $B = 0$ T case.

In all the previous figures, the most meaningful consequence of the magnetic field is the displacement of the positions at which the magnitudes analysed take their maxima values. The reason for this is that the effect of the magnetic field has been taken into account only via the gap of the material according to equation (8).

In figure 8, the third-order cross-section is presented. Here, we have a situation analogous to the previous case. However, there is a displacement of the curves of the order of one phonon, while the magnitude of $\sigma/\Lambda_1\Gamma_1$ remains the same.

Starting from the spectra of an effective section, we can obtain information about the characteristic parameters of the material, such as: the characteristic frequencies for which the material absorbs or emits a photon; the energy gaps; the energy of the optical phonons of the material; the exciton–phonon coupling constant; and the Landé g-factor.

References

[1] Brandt N B and Moshchalkov V V 1984 *Adv. Phys.* **33** 193
[2] Furdyna J K 1982 *J. Appl. Phys.* **53** 7637
[3] Takeyama S, Adachi S, Takagi Y and Aguekian V F 1995 *Phys. Rev.* B **51** 4858
[4] Golnik A, Ginter J and Gaj J A 1983 *J. Phys. C: Solid State Phys.* **16** 6073
[5] Wolff P A 1988 Diluted magnetic semiconductors *Semiconductors and Semimetals* vol 25, ed J K Furdyna and J Kossut (London: Academic) p 413
[6] Leite R C C, Scott J F and Damen T C 1969 *Phys. Rev. Lett.* **22** 780
[7] Gross E, Permogorov S, Travnikov V and Selkin A 1970 *J. Phys. Chem. Solids* **31** 2595
[8] Planel R, Bonnot A and Benoit à la Guillaume G 1973 *Phys. Status Solidi* b **58** 251
[9] Gross E, Permogorov S, Morozenko Y A and Kharlamov B 1973 *Phys. Status Solidi* b **59** 551
[10] Yoshida M, Ohno N, Mitsutake H, Nakamura K and Nakai Y 1985 *J. Phys. Soc. Japan* **54** 2754
[11] Ohno N, Yoshida M, Nakamura K and Nakai Y 1985 *Solid State Commun.* **53** 569
[12] Riera R, Sotolongo O and Lang I G 1991 *Phys. Status Solidi* b **165** 649
[13] Riera R, Rosas R, Marín J L and Sotolongo O 1998 *Phys. Status Solidi* b **207** 393
[14] Trallero-Giner C, Likawa F and Cardona M 1991 *Phys. Rev.* B **44** 12815
[15] Limmer W, Bauer S, Leiderer H, Gebhardt W, Cantarero A, Trallero-Giner C and Cardona M 1992 *Phys. Rev.* B **45** 11709
[16] Trallero-Giner C and Riera R 1989 *Phys. Status Solidi* b **152** 357
[17] Gaj J A, Ginter J and Galazka R R 1978 *Phys. Status Solidi* b **89** 655
[18] Gaj J A, Planel R and Fishman G 1979 *Solid State Commun.* **29** 435
[19] Gubarev S I, Ruf T and Cardona M 1991 *Phys. Rev.* B **43** 1551
[20] Goltsev A G, Lang I G, Pavlov S T and Bryzhina M F 1983 *J. Phys. C: Solid State Phys.* **21** 4221
[21] Pollak F H and Cardona M 1968 *Phys. Rev.* **172** 816
[22] Trallero-Giner C, Ruf T and Cardona M 1990 *Phys. Rev.* **41** 3028
[23] Ivchenko E L, Lang I G and Pavlov S T 1977 *Fiz. Tverd. Tela* **19** 1227, 2751 (Engl. transl. *Sov. Phys.–Solid State* **19** 718)
Ivchenko E L, Lang I G and Pavlov S T 1978 *Phys. Status Solidi* b **85** 81
[24] Trallero-Giner C, Lang I G and Pavlov S T 1980 *Phys. Status Solidi* b **100** 631
[25] Trallero-Giner C, Lang I G and Pavlov S T 1981 *Fiz. Tverd. Tela* **23** 1265
[26] Aristova K A, Trallero-Giner C, Lang I G and Pavlov S T 1978 *Phys. Status Solidi* b **85** 351
[27] Elliot R J 1957 *Phys. Rev.* **108** 1384
[28] Trallero-Giner C, Lang I G and Pavlov S T 1979 *Fiz. Tverd. Tela* **21** 2028 (Engl. transl. 1979 *Sov. Phys.–Solid State* **21** 1163)
[29] Landau L D and Lifshitz E M 1977 *Quantum Mechanics (Course of Theoretical Physics vol 3)* (Oxford: Pergamon) p 117
[30] Cantarero A, Trallero-Giner C and Cardona M 1989 *Phys. Rev.* B **39** 8388
[31] Trallero-Giner C, Cantarero A and Cardona M 1989 *Phys. Rev.* B **40** 4030